

U.S. Department of the Interior
U.S. Geological Survey

Reservoir Quality and Diagenetic Evolution of Upper Mississippian Rocks in the Illinois Basin: Influence of a Regional Hydrothermal Fluid-Flow Event During Late Diagenesis

U.S. Geological Survey Professional Paper 1597

Availability of Publications of the U.S. Geological Survey

Order U.S. Geological Survey (USGS) publications from the offices listed below. Detailed ordering instructions, along with prices of the last offerings, are given in the current-year issues of the catalog "New Publications of the U.S. Geological Survey."

Books, Maps, and Other Publications

By Mail

Books, maps, and other publications are available by mail from—

USGS Information Services
Box 25286, Federal Center
Denver, CO 80225

Publications include Professional Papers, Bulletins, Water-Supply Papers, Techniques of Water-Resources Investigations, Circulars, Fact Sheets, publications of general interest, single copies of permanent USGS catalogs, and topographic and thematic maps.

Over the Counter

Books, maps, and other publications of the U.S. Geological Survey are available over the counter at the following USGS Earth Science Information Centers (ESIC's), all of which are authorized agents of the Superintendent of Documents:

- Anchorage, Alaska—Rm. 101, 4230 University Dr.
- Denver, Colorado—Bldg. 810, Federal Center
- Menlo Park, California—Rm. 3128, Bldg. 3, 345 Middlefield Rd.
- Reston, Virginia—Rm. 1C402, USGS National Center, 12201 Sunrise Valley Dr.
- Salt Lake City, Utah—2222 West, 2300 South (books and maps available for inspection only)
- Spokane, Washington—Rm. 135, U.S. Post Office Building, 904 West Riverside Ave.
- Washington, D.C.—Rm. 2650, Main Interior Bldg., 18th and C Sts., NW.

Maps only may be purchased over the counter at the following USGS office:

- Rolla, Missouri—1400 Independence Rd.

Electronically

Some USGS publications, including the catalog "New Publications of the U.S. Geological Survey" are also available electronically on the USGS's World Wide Web home page at <http://www.usgs.gov>

Preliminary Determination of Epicenters

Subscriptions to the periodical "Preliminary Determination of Epicenters" can be obtained only from the Superintendent of

Documents. Check or money order must be payable to the Superintendent of Documents. Order by mail from—

Superintendent of Documents
Government Printing Office
Washington, DC 20402

Information Periodicals

Many Information Periodicals products are available through the systems or formats listed below:

Printed Products

Printed copies of the Minerals Yearbook and the Mineral Commodity Summaries can be ordered from the Superintendent of Documents, Government Printing Office (address above). Printed copies of Metal Industry Indicators and Mineral Industry Surveys can be ordered from the Center for Disease Control and Prevention, National Institute for Occupational Safety and Health, Pittsburgh Research Center, P.O. Box 18070, Pittsburgh, PA 15236-0070.

Mines FaxBack: Return fax service

1. Use the touch-tone handset attached to your fax machine's telephone jack. (ISDN [digital] telephones cannot be used with fax machines.)
2. Dial (703) 648-4999.
3. Listen to the menu options and punch in the number of your selection, using the touch-tone telephone.
4. After completing your selection, press the start button on your fax machine.

CD-ROM

A disc containing chapters of the Minerals Yearbook (1993-95), the Mineral Commodity Summaries (1995-97), a statistical compendium (1970-90), and other publications is updated three times a year and sold by the Superintendent of Documents, Government Printing Office (address above).

World Wide Web

Minerals information is available electronically at <http://minerals.er.usgs.gov/minerals/>

Subscription to the catalog "New Publications of the U.S. Geological Survey"

Those wishing to be placed on a free subscription list for the catalog "New Publications of the U.S. Geological Survey" should write to—

U.S. Geological Survey
903 National Center
Reston, VA 20192

Reservoir Quality and Diagenetic Evolution of Upper Mississippian Rocks in the Illinois Basin: Influence of a Regional Hydrothermal Fluid-Flow Event During Late Diagenesis

By Janet K. Pitman, Mitchell Henry, *and* Beverly Seyler

U.S. GEOLOGICAL SURVEY PROFESSIONAL PAPER 1597



UNITED STATES GOVERNMENT PRINTING OFFICE, WASHINGTON : 1998

U.S. DEPARTMENT OF THE INTERIOR

BRUCE BABBITT, Secretary

U.S. GEOLOGICAL SURVEY

Thomas J. Casadevall, Acting Director

For sale by U.S. Geological Survey, Information Services
Box 25286, Federal Center
Denver, CO 80225

Any use of trade, product, or firm names in this publication is for descriptive purposes only and does not imply endorsement by the U.S. Government

Library of Congress Cataloging-in-Publication Data

Pitman, Janet K.

Reservoir quality and diagenetic evolution of Upper Mississippian rocks in the Illinois Basin : Influence of a regional hydrothermal fluid-flow event during late diagenesis / by Janet K. Pitman, Mitchell Henry, and Beverly Seyler.

p. cm.—(U.S. Geological Survey professional paper : 1597)

Includes bibliographical references.

Supt. of docs. no. : I 19.16 : 1597

1. Sandstone—Illinois Basin. 2. Petroleum—Geology—Illinois Basin.
3. Geology, Stratigraphic—Mississippian. 4. Diagenesis—Illinois Basin.

I. Henry, Mitchell E. II. Seyler, Beverly. III. Title. IV. Series

QE471.15.S25P57 1999

553.2'82—dc21

98-6426

CIP

CONTENTS

Abstract.....	1
Introduction	1
Geologic and Depositional History	2
Methods	3
Reservoir Characteristics	6
Porosity	6
Permeability	7
Porosity/Permeability Relationships and Distribution Patterns	8
Controls on Reservoir Quality	8
General Statement	8
Detrital Mineralogy	8
Mineral Diagenesis	10
Compaction Features	10
Secondary Quartz	10
Carbonate Cements.....	10
Authigenic Clay Minerals.....	16
Other Phases	16
Secondary Porosity.....	16
Evolution of Reservoir Quality	18
Quartz Cementation	18
Carbonate Diagenesis	18
Clay Mineral Precipitation	20
Secondary Porosity Development	20
Generation and Migration of Petroleum	21
Thermal and Hydrologic Controls on Diagenesis	21
Conclusions	22
Acknowledgments	23
References Cited	23

FIGURES

1. Location map of the Illinois Basin.....	2
2. Generalized lithologic section of Mississippian strata in the southern Illinois Basin	3
3. Map showing location of wells sampled for petrographic and geochemical analysis	4
4–8. Graphs of:	
4. Relationship between core porosity and permeability for sandstones within the Bethel-Cypress interval	6
5. Core porosity versus depth for reservoir sandstones	6
6. Relationship between compactional and cementational porosity loss in reservoir sandstones	7
7. Intergranular volume versus percent thin-section porosity in sandstones within the Cypress	7
8. Permeability versus depth for reservoir sandstones.....	8
9. Isocontour maps depicting regional variations in core porosity and permeability in sandstones within the Bethel-Cypress interval.....	9
10. Map showing late-diagenetic quartz and ankerite cementation relative to faults in southern Illinois	10
11. Chart showing paragenetic sequence of diagenetic events in reservoir sandstones.....	11
12. Ternary QFL plots for sandstones from the Bethel and Cypress	11

13. Graph showing stable isotope compositions of diagenetic carbonate cements in reservoir sandstones.....	16
14. Burial and thermal history curves for the Bethel Sandstone–Cypress Sandstone interval showing relative timing of major diagenetic events in southern and central Illinois	17
15. Graphs showing equilibrium relationships between $\delta^{18}\text{O}$ of water, $\delta^{18}\text{O}$ of calcite and ankerite, and crystallization temperature.....	19

TABLES

1. Locations of wells sampled for petrographic and geochemical analysis.....	5
2. Mineralogic composition of sandstones within the Bethel-Cypress interval	12
3. Stable isotope compositions of carbonate cements in sandstones within the Bethel-Cypress interval	15

Reservoir Quality and Diagenetic Evolution of Upper Mississippian Rocks in the Illinois Basin: Influence of a Regional Hydrothermal Fluid-Flow Event During Late Diagenesis

By Janet K. Pitman,¹ Mitchell Henry,¹ and Beverly Seyler²

ABSTRACT

Reduction and enhancement of porosity due to diagenetic alterations are common in Upper Mississippian Bethel and Cypress Sandstones in the Illinois Basin. Reduced porosity was caused by mechanical compaction and cementation by carbonate and quartz overgrowths. Enhanced porosity is mostly of secondary origin due to cement and framework grain dissolution, with only minor primary porosity preserved by early grain-rimming clay. Secondary porosity was caused by acidic meteoric waters and deep basin brines carrying organic and inorganic acids released during maturation of the Upper Devonian and Lower Mississippian New Albany Shale in the Early Permian. Burial-history reconstruction suggests that sandstone diagenesis took place over a short time interval culminating in the Late Pennsylvanian to Early Permian when the rocks were at or close to their maximum burial (~2 km). Major diagenetic events observed in sandstones include (1) precompactional illite and early chlorite precipitation, (2) early quartz, and calcite and dolomite cementation, (3) calcite-cement and framework-grain dissolution, (4) illite and kaolinite formation, (5) late quartz and ankerite precipitation, (6) fracture cementation, and (7) hydrocarbon emplacement. On the basis of stable-isotope data and thermal modeling, early diagenetic nonferroan carbonate and quartz cement precipitated in a shallow meteoric environment governed by burial heat flow. In contrast, late-diagenetic ferroan carbonate, anhydrite, and quartz cementation occurred in a regime influenced by advective (hydrothermal) fluid flow. In southern Illinois, combined igneous and hydrothermal heat transport during the late Paleozoic increased the rate of hydrocarbon expulsion, which resulted in the migration of large amounts of petroleum into reservoir sandstones.

¹U.S. Geological Survey, Mail Stop 939, Box 25046, Denver, Colorado, 80225.

²Illinois State Geological Survey, 615 East Peabody Dr., Champaign, Illinois, 61820.

INTRODUCTION

Sixty percent of the oil produced in the Illinois Basin comes from Upper Mississippian rocks, and most of this production is from sandstones. Rocks of Mississippian age are limited to the southern half of Illinois, southwestern Indiana, and western Kentucky and reach their maximum thickness, about 430 m, in southern Illinois (fig. 1). This study examines the controls on reservoir quality and delineates general reservoir-quality trends, as governed by porosity and permeability in the Mississippian Bethel and Cypress Sandstones, two of the principal producing units in the Illinois Basin. Identifying the major influences on porosity and permeability distribution provides insight into some of the processes that must be accounted for in developing reliable porosity prediction models. Overall, sandstones within the Bethel-Cypress interval have good porosity and permeability. In the main reservoir units, porosity varies from 10 to 25 percent, with permeabilities ranging over about four orders of magnitude (<1–2,500 mD) at any given depth.

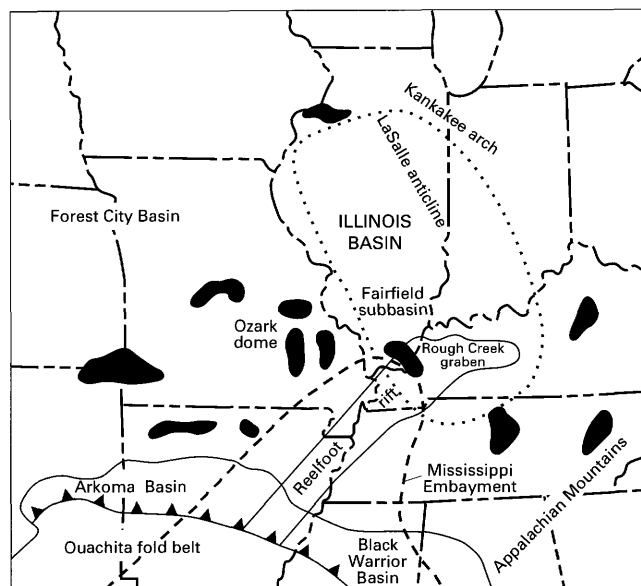
In the Illinois Basin, the reservoir quality in shallowly buried sandstones (<500 m) generally is high, but, in moderately buried sandstones (>500 m), reservoir quality can be quite variable because of extensive alteration. Reduction in porosity in sandstones is due primarily to mechanical compaction and the formation of quartz and carbonate cement; porosity enhancement is a result of carbonate- and framework-grain dissolution. Permeability variations at any given depth are a function of porosity, cement volume, and fracture development. In this study, petrographic and geochemical analysis is used to decipher the diagenetic controls on reservoir quality and the timing of diagenesis relative to migration and entrapment of hydrocarbons. An additional aspect of the study involves linking inorganic and organic diagenesis to late Paleozoic tectonic and hydrothermal fluid-flow events in the region. Some of these parameters are difficult to evaluate, but an understanding of their potential should enhance reservoir-quality prediction in undrilled areas of the basin.

GEOLOGIC AND DEPOSITIONAL HISTORY

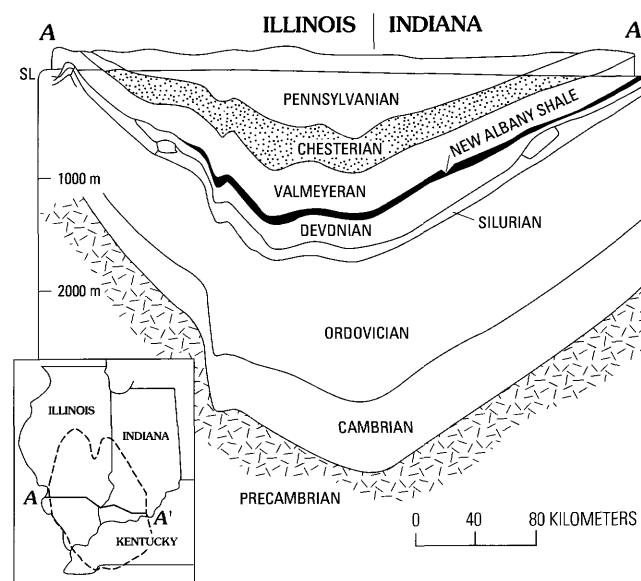
In the Illinois Basin, the (Upper Mississippian) Bethel and Cypress Sandstone interval is part of the lower Chesterian Series in the upper part of the Kaskaskia sequence (Swann, 1963). Stratigraphic relations for the Upper Mississippian are shown in figure 2. The Chesterian Series consists of alternating sandstone, shale, and limestone beds that record cyclic sedimentation in response to sea-level changes during the Mississippian (Pryor and Sable, 1974). Chesterian-age rocks together with sandstone and fossiliferous carbonate units in the upper part of the Valmeyeran Series are the principal reservoirs for most of the oil produced in the basin.

The geology and sedimentology of the Chesterian Series are given in Treworgy (1991) and Willman and others (1975). The Bethel and Cypress Sandstones represent facies of a large southeasterly prograding fluvial-deltaic system that deposited sediment shed from the eastern Canadian Shield. The Bethel Sandstone thickens downdip to more than 30 m in southeastern Illinois and 75 m in western Kentucky (Sullivan, 1972). The facies is composed of tidal-dominated, deltaic to shallow-marine deposits that commonly display a northeast-southwest trend, as do other Chesterian-age units in the basin (Treworgy, 1991). The Cypress Sandstone is more than 30 m thick, locally reaching as much as 60 m in the south-central part of the Illinois Basin (Willman and others, 1975). Depositional facies in the Cypress include distributary-bar, point-bar, and marine-sheet-sandstone deposits that are discontinuous and aligned parallel to major structural features in the basin (Pryor and others, 1991). Throughout the area of deposition, the Cypress Sandstone is conformably overlain by the Beech Creek Limestone, a widespread reservoir seal for Cypress Sandstone traps. The Cypress has been eroded along the southeast margin of the basin.

The Illinois Basin experienced periodic subsidence and multiple episodes of uplift and erosion before and after deposition of the Chesterian Series in Late Mississippian time. In southern Illinois, burial-history modeling indicates that maximum burial of Upper Mississippian strata was attained when the rocks reached depths of approximately 2 km during the Late Pennsylvanian to Early Permian. Somewhat lower maximum burial depths were reached near the Chesterian Series subcrop in central Illinois. During the Late Pennsylvanian to Early Permian, local igneous activity and compressional stresses associated with the Ouachita orogeny caused extensive folding and faulting, which resulted in the development of many of the structural traps in the basin. Erosion accompanied late Paleozoic uplift and was particularly widespread along the southeastern flank of the basin. Near-surface coal beds in Pennsylvanian strata across the basin display anomalously high thermal maturities (Damburger, 1971; Cluff and Brynes, 1991), which suggest that at one time they were more deeply buried. On the basis of thermal modeling and



A



B

Figure 1. A, Location map showing the Illinois Basin. Black areas are ore districts. B, East-west cross section depicting the Upper Mississippian Chesterian Series and Upper Devonian and Lower Mississippian New Albany Shale; the subcrop of the Chesterian Series is shown as a dashed line on inset map (modified from Swann, 1967).

biomarker studies, the amount of section removed during erosion was approximately 1 km in southern Illinois, decreasing to several hundreds of meters in central Illinois (Rowan and others, in press). Although somewhat lower than the amount reported in others studies (1,400 m, Damburger, 1971; 2,000 m, Cluff and Brynes, 1991), the estimated erosional loss is within the range of realistic values.

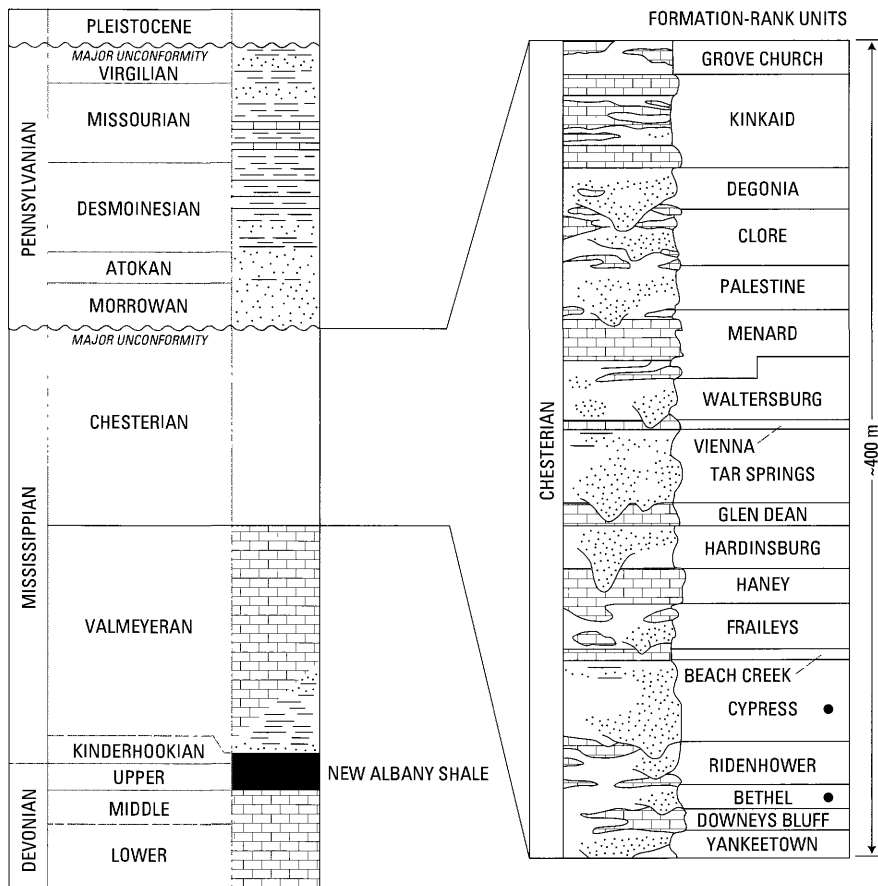


Figure 2. Generalized lithologic section of Mississippian strata in the southern Illinois Basin (modified from Swann, 1963). Black dots indicate units analyzed in this study.

METHODS

Approximately 150 samples of core from 82 wells penetrating the Bethel-Cypress interval were collected from Illinois and Indiana for petrographic analysis (fig. 3; table 1). API location data, shown on table 1, were taken from the Illinois State Geological Survey's well inventory system. In Illinois, wells chosen for study in the Bethel Sandstone span a depth interval of 365 to 853 m; wells in the Cypress Sandstone that were sampled ranged from 305 to 884 m. Some sandstone samples in Indiana were at depths of only a few meters to several tens of meters below the surface.

To facilitate analysis, thin sections of individual sandstones were impregnated with blue epoxy for porosity identification and stained for mineral identification. Staining with Alizarin red-S and potassium ferricyanide permitted Fe-free and Fe-bearing carbonate minerals to be readily distinguished; sodium cobaltinitrate stain aided in the identification of K-feldspar. Routine point counts (300 grains per sample) were performed on each sample to quantify rock composition and thin-section porosity. Mineralogical classification of the data is based on Folk (1974). In this study, the quartz category was modified to consist of only monocrystalline grains; polycrystalline

quartz grains were included as rock fragments. Grain size, based on the apparent long axis of framework grains, was determined for each sample.

In addition to petrographic analysis, representative sandstone samples were analyzed isotopically by Global Geochemistry (Canoga Park, Calif.) and Mountain Mass Spectrometry (Evergreen, Colo.). Carbon and oxygen isotope ratios were obtained by a timed-dissolution procedure based on different reaction rates for chemically distinct carbonate phases (Walters and others, 1972). To prevent contamination from organic matter during acid digestion, kerogen was removed from the samples prior to analysis. Upon reaction with phosphoric acid, CO_2 gas evolved in the first hour was attributed to calcite and CO_2 gas evolved after several hours was assigned to dolomite. All isotope results are reported as the per mill (‰) difference relative to the PDB standard using the delta (δ) notation. Data reproducibility is precise to $\pm 0.2\text{‰}$.

Conventional porosity and permeability data, provided by the Illinois and Indiana State Geological Surveys, were compiled in a reservoir-property database. Porosity analysis of individual core samples was performed by helium injection in a porosimeter using the Boyle's gas law method under ambient, or near-ambient, conditions. Permeability

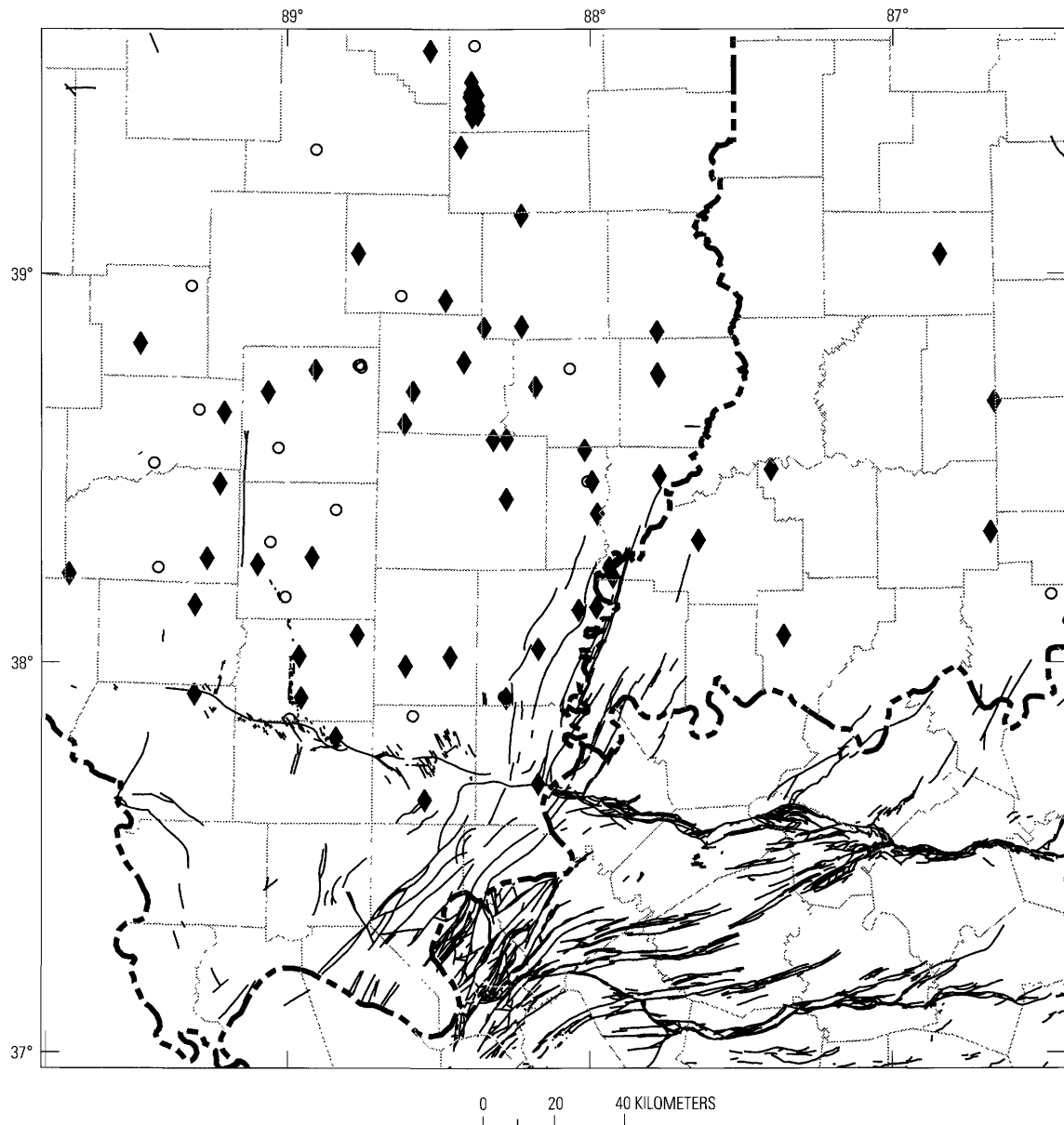


Figure 3. Map showing location of wells sampled for petrographic and geochemical analysis. Diamond symbols denote Cypress Sandstone samples, circles correspond to Bethel Sandstone samples.

measurements were made using nitrogen gas or air as the fluid. Wells incorporated in the database were selected to cover as wide a geographic area as possible. The porosity and permeability for each well were averaged as a whole rather than as individual facies because of complex lithogenetic relationships that are commonly difficult to distinguish on well logs and in drill cores. To minimize the potentially large effects of anomalous porosity and permeability on averages, median rather than mean porosity and permeability values were determined. The contribution of natural fractures to effective reservoir permeability was beyond the scope of the study.

Combined burial- and temperature-history curves (modified from Rowan and others, in press) were constructed for the Bethel-Cypress stratigraphic interval in the southern

Illinois Basin using the two-dimensional, finite-difference program, Basin2. The model takes into account differences in deposition and erosion, porosity and permeability variations, and the thermal effects of fluid flow during the basin's history. Thermal and petrographic data constrained the amount of uplift and erosion in the model to ~1 km. Coupled numerical fluid- and heat-flow calculations were used by Basin2 to produce a paleotemperature profile that reconciled observed biomarker and vitrinite reflectance maturities and measured fluid-inclusion homogenization temperatures. A temperature profile based on burial heat flow alone was constructed for comparison. The accuracy of the modeling results is subject to uncertainties involved in age determinations of stratigraphic intervals, amounts of erosion, and variations in heat flow.

Table 1. Location of wells sampled for petrographic and geochemical analysis.

[Latitude in decimal degrees north; longitude in decimal degrees west]

Core ID	API no.	Latitude	Longitude	Core ID	API no.	Latitude	Longitude
Bethel Sandstone				C01103	1218900387	38.277920	89.247419
C0071	1207700603	37.928828	89.283433	C01113	1218900176	38.470347	89.210327
C0285	1214502037	38.158661	89.285138	C01135	1207900014	39.164720	88.233602
C0318	1216501136	37.878645	88.578628	C01160	1208100552	38.282282	88.908279
C0345	1208102322	38.320668	89.042866	C01183	1219306873	37.926202	88.278548
C0361	1204700033	38.481371	88.014630	C01309	1218500599	38.496459	87.780426
C0364	1202702511	38.518618	89.424022	C01353	1204700182	38.398650	87.983098
C0414	1202900030	39.595217	88.388347	C01439	1208100764	38.263679	89.085271
C0467	1219304604	38.160159	87.986364	C01445	1219101791	38.589686	88.279198
C0468	1219306807	37.929945	88.285574	C01511	1204900140	39.065321	88.765539
C0518	1202700823	38.658891	89.278940	C01546	1202500525	38.789958	88.419539
C0525	1200500212	38.978035	89.309814	C01558	1202901169	39.469611	88.379941
C0573	1202500986	38.772606	88.753333	C01698	1202900325	39.460276	88.396417
C0595	1204900704	38.958267	88.624839	C01704	1202900291	39.420342	88.376784
C0597	1207900017	38.878071	88.352995	C01717	1202901131	39.463975	88.403436
C0607	1205500336	37.867485	88.975637	C01735	1202901134	39.474788	88.400756
C0651	1218900150	38.252045	89.403828	C01740	1202901301	39.433612	88.398575
C0735	1212101296	38.705799	89.055451	C01760	1202900795	39.427991	88.393260
C1018	1212104149	38.561675	89.020984	C01794	1202901319	39.437038	88.386898
C1113	1218900176	38.470347	89.210327	C01806	1202900869	39.414467	88.395643
C1125	1212590017	38.772307	88.073440	C01813	1203500074	39.337077	88.433253
C1169	1217300051	39.326445	88.906719	C01834	1202901353	39.442305	88.377306
C1270	1208100499	38.405546	88.831430	C01931	1202901019	39.502063	88.398420
C1511	1204900140	39.065321	88.765539	C01968	1202901330	39.433810	88.380040
C2069	1212101475	38.778051	88.762495	C01975	1202900788	39.424176	88.386237
C2085	1212104968	38.779868	88.755532	C01981	1207900301	38.881033	88.230995
C2114	1202500549	38.710497	88.584495	C02114	1202500549	38.710497	88.584495
C2230	1200500567	38.827081	89.474212	C02149	1219101213	38.435874	88.278806
C2341	1208100199	38.181586	88.992598	C02174	1204900813	38.946928	88.480065
IN303	No Data	38.185565	86.508559	C02230	1200500567	38.827081	89.474212
IN643	No Data	38.345879	86.704695	C02357	1212101986	38.765089	88.902172
Cypress Sandstone				C02621	1205901062	37.704520	88.173993
C00071	1207700603	37.928828	89.283433	C05279	1218502475	38.260543	87.944239
C00285	1214502037	38.158661	89.285138	C05834	1202501165	38.627951	88.610797
C00374	1219901289	37.820457	88.825271	C05874	1218900972	38.233049	89.690740
C00385	1215900044	38.725340	88.185230	C06058	1219302857	38.053129	88.174550
C00467	1219304604	38.160159	87.986364	C06079	1203307971	38.867555	87.788940
C00491	1205500563	38.029849	88.946832	C14018	1210127623	38.753134	87.783338
C00520	1204700028	38.481310	87.999950	C14019	1210128363	38.759770	87.786930
C00592	1219300424	38.153027	88.043539	C14023	1204724183	38.562076	88.025117
C00597	1207900017	38.878071	88.352995	IN071	No Data	38.086299	87.381803
C00642	1206502267	38.006169	88.605524	IN097	No Data	38.681153	86.687115
C00671	1205500350	38.085232	88.760615	IN133	No Data	38.238589	87.932857
C00693	1205500244	37.922344	88.939580	IN643	No Data	38.345879	86.704695
C00735	1212101296	38.705799	89.055451	IN647	No Data	38.330681	87.65548
C00962	1216502428	37.661006	88.539391	IN734B1	No Data	38.511973	87.418606
C00996	1219105483	38.588268	88.322813	IN745	No Data	39.062193	86.85704
C01049	1213900006	39.581258	88.534095				
C01096	1202700576	38.65244	89.198733				

RESERVOIR CHARACTERISTICS

POROSITY

Whole-core porosity in sandstones within the Bethel-Cypress interval varies by as much as 25 percent, with the majority of samples ranging from ~13 to 22 percent (fig. 4). Porosity/depth trends of sandstones within the Bethel-Cypress interval (fig. 5) depict a systematic decrease in median core porosity with increasing depth of burial. The relationship between porosity and burial depth generally is assumed to be exponential (e.g., Baldwin and Butler, 1985); however, given the limited depth range of the available data, a simple linear trend is a good approximation. Regression analysis of the sandstone data shows that core porosity decreases approximately 15 percent between 400 and 1,000 m. Porosity values that fall to the right of the trend line (at depths >~750 m in fig. 5) reflect various amounts of erosion in different areas of the basin or the effects of diagenesis and mechanical compaction. These variations in core porosity also could reflect differences in framework grain size, shape, and sorting related to depositional-energy conditions and sediment source.

Measured whole-core porosities for sandstones within the Bethel-Cypress interval (~5–25 percent) compare very closely with the observed porosities in thin section (<1–25 percent). Generally, thin-section porosities tend to be lower because of the difficulty in quantifying microporosity. Most visible porosity in thin section is macroporosity, thus the difference between core and thin-section porosity provides an estimate of the amount of microporosity in a sample. In Mississippian sandstones, average core porosity differs from thin-section porosity by <5 percent, suggesting that microporosity (mostly associated with authigenic and detrital clay) is quantitatively insignificant. It is important to note that thin-section porosity in sandstones within the Bethel-Cypress interval does not vary with differences in grain size, nor does it show a depth-related trend as does core porosity. The latter is probably due to the limited size of the data set.

Intergranular volume (IGV), which is the sum of intergranular porosity plus mineral cements (Houseknecht, 1987), is a means of evaluating the relative importance of compaction versus cementation in initial porosity loss in sandstones. The IGV's in all sandstones within the Bethel average 21 percent; sandstones within the Cypress average 26 percent IGV (fig. 6). Most sandstones within the Bethel-Cypress interval are very fine to medium grained (~70–380 μm) and moderately to well sorted with <5 percent detrital clay. Studies show that initial porosities of well-sorted sandstones are approximately 40 percent (Beard and Weyl, 1973; Atkins and McBride, 1992; Ehrenberg, 1995). Assuming an estimated 40 percent depositional porosity in sandstones within the Bethel-Cypress interval, an average of 47 percent of the original porosity in the Bethel was reduced by compaction,

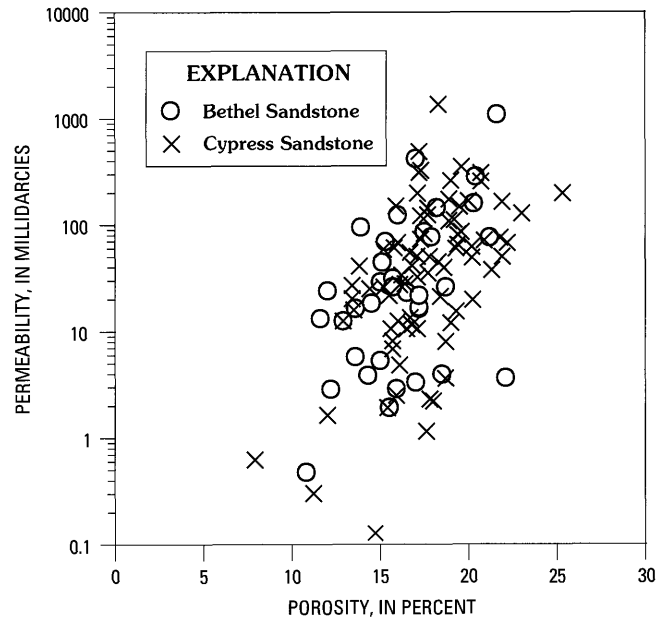


Figure 4. Relationship between core porosity and permeability for the sandstones within the Bethel-Cypress interval.

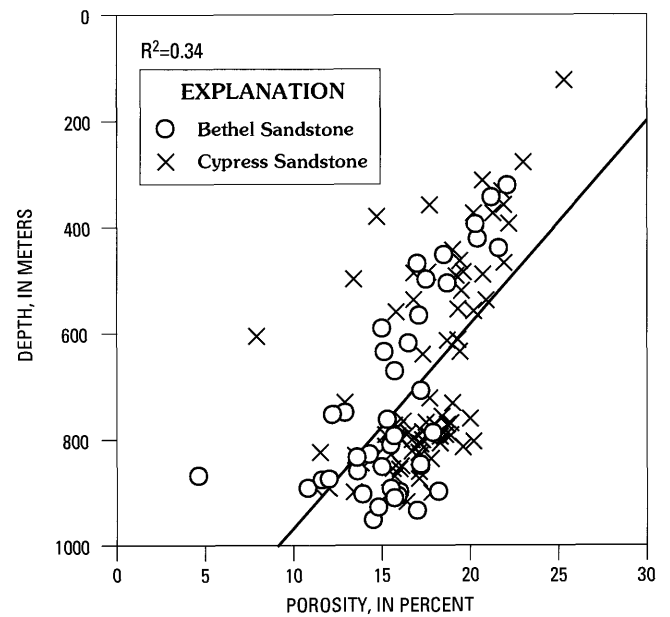


Figure 5. Plot of core porosity versus depth for reservoir sandstones. Note that porosity decreases with increasing depth. R^2 corresponds to correlation coefficient.

and an additional 29 percent was lost by quartz and carbonate cementation (fig. 6). In the sandstones within the Cypress, 34 percent of the porosity was lost by compaction and 34 percent by cementation. An average of about 9 percent secondary porosity in the Bethel Sandstone and 13 percent in the Cypress Sandstone was generated by carbonate-cement and minor framework-grain dissolution during later burial. The

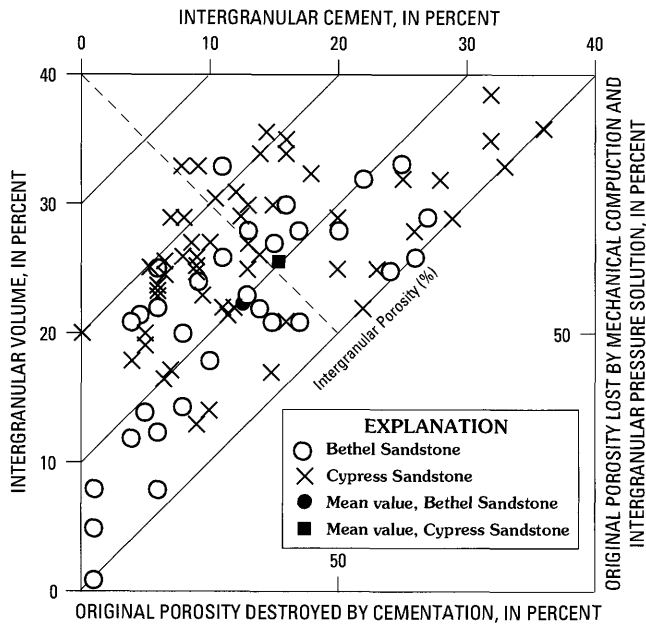


Figure 6. Relationship between compactional and cementational porosity loss in reservoir sandstones (after Houseknecht, 1987).

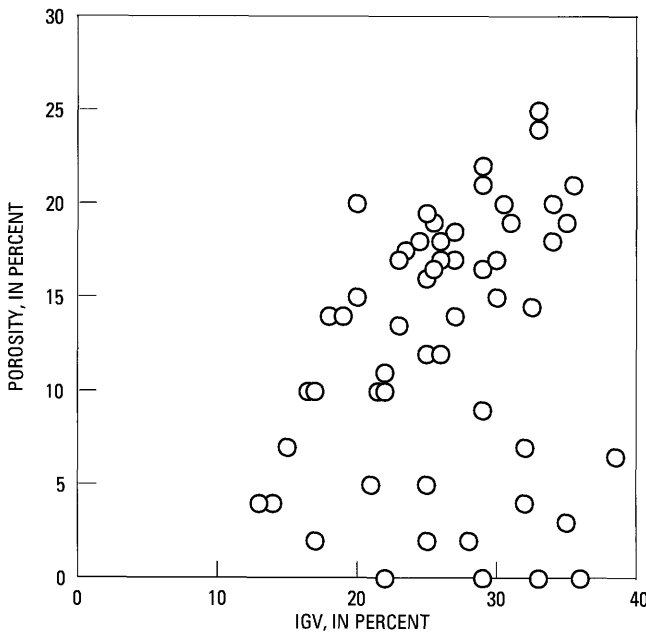


Figure 7. Plot showing percent intergranular volume (IGV) versus percent thin-section porosity in sandstones within the Cypress.

processes controlling porosity reduction are consistent with the mineralogic and textural differences observed in thin section. Petrographic analysis indicates that, during early burial, mechanical compaction was the main porosity-reducing process; however, as burial increased, mechanical compaction and mineral cementation were of approximately equal importance in reducing reservoir quality. A comparison of IGV versus thin-section porosity in sandstones within

the Cypress (fig. 7) shows no apparent trend with increasing porosity—this confirms petrographic observation that, despite IGV's varying from 13 to 38 percent (average 26 percent), low-porosity (cemented) sandstones are no more or less compacted than are the high-porosity sandstones. According to Stone and others (1993) and Stone and Siever (1994), IGV stabilizes at 24–26 percent between depths of 1.5 and 2.5 km in quartz-rich sandstones. The average IGV in the Bethel Sandstone (21 percent) is slightly lower than the range of values (24–26 percent) that represents the configuration that typically can be reached by rearrangement of rigid grains at closest packing. Reduction of IGV below this value suggests that minor intergranular pressure solution, as observed in some sandstones, allowed framework grains to fit into a tighter packing arrangement. Variations in reservoir quality in sandstones within the Bethel-Cypress interval thus resulted from a combination of physical and diagenetic modifications at shallow to moderate burial depths.

PERMEABILITY

The positive correlation between core porosity and permeability in sandstones within the Bethel-Cypress interval (see fig. 4) suggests that the primary control on permeability is porosity, although other variables also can affect permeability. Some scatter in the permeability data may be artificial, caused by measurements made on samples containing coring-induced hairline fractures. Unfortunately, these samples were not available for examination; thus, the presence of unnatural fractures could not be fully evaluated. It is also important to note that total porosity does not distinguish a sample with mostly primary porosity from one that contains dominantly secondary porosity. Petrographic observations show that primary pores have better connectivity than secondary pores, resulting in a greater contribution to permeability.

Unlike porosity, permeability in sandstones within the Bethel-Cypress interval is unrelated to depth and varies markedly at any given depth (fig. 8). Substantial variations in permeability with depth are related to a number of parameters besides porosity, including variations in grain size and sorting, total cement volume, and primary and secondary porosity. Assuming the same degree of sorting, coarser grained sandstones would be expected to have higher permeability at the time of deposition than would finer grained sandstones (Beard and Weyl, 1973). The Bethel and Cypress Sandstones have undergone substantial diagenesis since they were deposited, but some of the original variations in permeability due to small grain size differences have been preserved.

Total cement volume is an important control on permeability in sandstones within the Bethel-Cypress interval and generally is a greater predictor of permeability than one or more authigenic mineral phases alone. Petrographic

observations suggest that increased amounts of carbonate and silica cement decreased permeability by occluding porosity and narrowing pore throats, particularly in primary intergranular pores. On the other hand, sandstones that have high amounts of quartz cement commonly have low permeability, but sandstones with low amounts of secondary quartz also can have low permeability because they contain abundant carbonate cement. The relationship between permeability and clay matrix in sandstones within the Bethel-Cypress interval is not well defined. Overall, permeability decreases with increasing detrital matrix content; however, low permeability commonly occurs in sandstones that have small amounts of matrix and large amounts of authigenic cement.

POROSITY/PERMEABILITY RELATIONSHIPS AND DISTRIBUTION PATTERNS

The relationship between median core porosity and median permeability for sandstones within the Bethel-Cypress interval (fig. 4) defines a linear decrease in porosity with the log of permeability. The significant overlap between these parameters suggests that similar depositional and diagenetic processes affected both units. Reservoir quality variations in the Bethel and Cypress are difficult to evaluate on a regional scale because of the lack of uniformly distributed porosity and permeability data across the study area; however, differences in porosity and permeability overall are of the same order of magnitude and basin-wide patterns in reservoir quality are generally comparable (fig. 9). The best porosity and permeability in both the Bethel and the Cypress occurs in the western portion of the area where values exceed 20 percent and 2 mD, respectively. The Cypress Sandstone also shows high porosity and permeability locally in the eastern part of the basin. Reservoir quality in both units decreases in sandstones downdip to <15 percent and <1 mD in the southern part of the basin. In downdip parts of the study area close to faults (see fig. 9), petrographic analysis indicates that porosity in the Cypress Sandstone is as low as a few percent because of extensive mechanical compaction and late diagenetic cementation. Away from faults, porosity increases to approximately 15 percent due to the development of secondary porosity. In both units, higher porosity and permeability correspond to increasing secondary porosity.

Fracture porosity, used here to denote open pore space within the plane of a fracture, is present, particularly along parts of some major fault systems. Although several core samples indicate that some faults have porosity, the extent to which faults and fractures are open and permeable requires analysis of well tests and field-performance data that is beyond the scope of this paper.

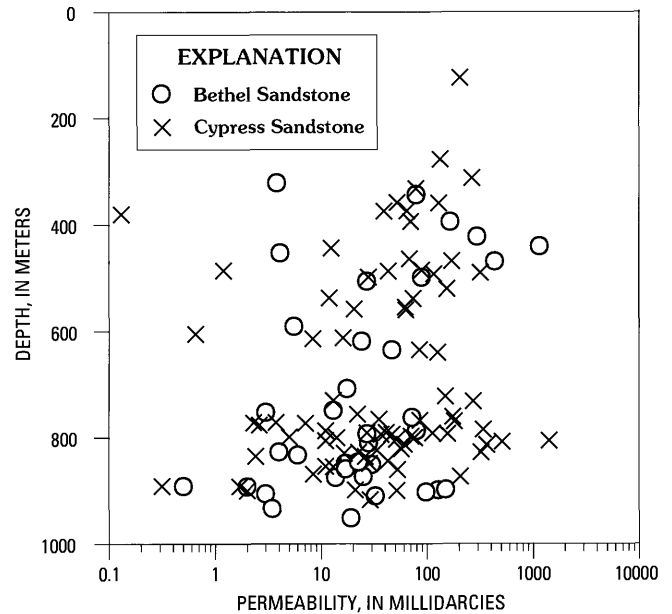


Figure 8. Plot of permeability versus depth for reservoir sandstones. Note that permeability is highly variable at any given depth.

CONTROLS ON RESERVOIR QUALITY

GENERAL STATEMENT

Regional controls on reservoir quality in sedimentary basins include depositional environment, initial framework grain composition, grain size and sorting, subsidence rate, pressure, temperature, pore-fluid composition, and diagenesis. In the Illinois Basin, reservoir quality in sandstones within the Bethel-Cypress interval is influenced primarily by (1) framework grain composition and (2) diagenesis. On a basin-wide scale, detrital and authigenic mineral suites show only minor differences in type and abundance and are depth independent. In addition, except for some late diagenetic phases that are locally restricted to the southern part of the basin (fig. 10), most detrital and authigenic minerals do not display systematic or regional variations. The paragenetic sequence of major diagenetic events in the Bethel-Cypress interval, as indicated by textural features, is shown in figure 11.

DETRITAL MINERALOGY

Sandstones within the Bethel-Cypress interval are subarkoses and sublitharenites with a combined average composition of 83 percent quartz, 8 percent feldspar, and 9 percent rock fragments or quartzarenites with >90 percent quartz (fig. 12; table 2). Quartz grains in sandstones typically are monocrystalline with optically continuous overgrowths and, in some samples, appear rounded, indicating they are reworked, second-cycle sediments. The feldspar content of

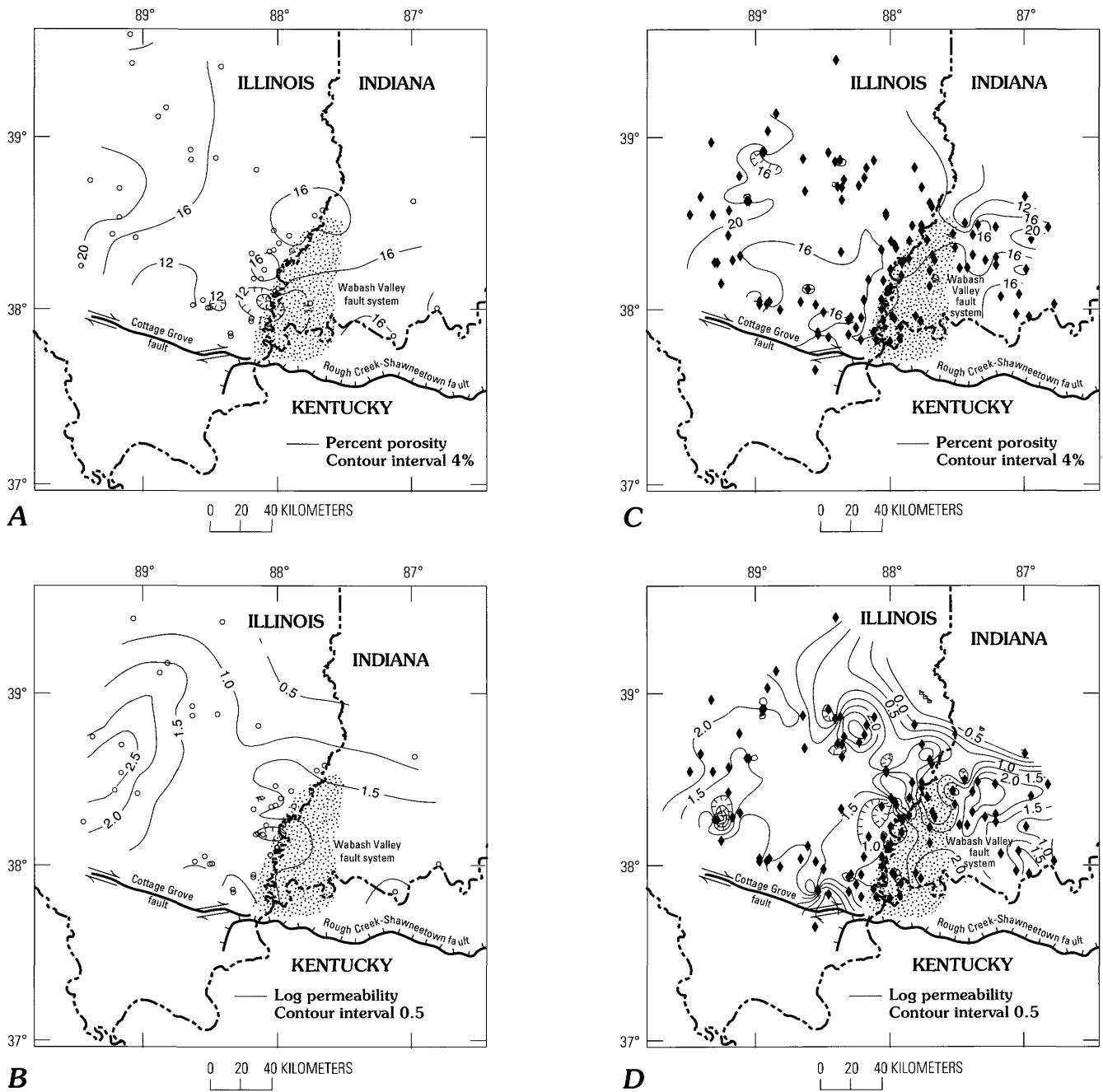


Figure 9. Isocontour maps depicting regional variations in reservoir quality in sandstones within the Bethel-Cypress interval. *A*, percent porosity, Bethel Sandstone; *B*, log permeability, Bethel Sandstone; *C*, percent porosity, Cypress Sandstone; *D*, log permeability, Cypress Sandstone. Stippled pattern indicates Wabash Valley fault system.

sandstones comprises approximately equal amounts of potassium and sodium varieties. Most potassium feldspar grains exhibit the effects of alteration, such as replacement by authigenic clay or, less commonly, ferroan carbonate. Many sandstones display honeycombed grains or moldic and oversized pores, indicating partial to complete K-feldspar(?) dissolution. Na-feldspar, dominantly plagioclase, may show clay alteration, but leaching tends to be minor. Lithic grains include plutonic and metamorphic polycrystalline quartz

and, less commonly, gneiss, chert, argillite, and carbonate intraclasts. The relative proportion of polycrystalline quartz grains generally increases with increasing grain size. Fossil bioclasts (included in total lithics category of table 2) are present locally in some sandstones and include a variety of bryozoan and echinoderm fragments; similar fossil types have been reported in the upper Valmeyeran Series (Pryor and others, 1991). Illitic clay matrix is confined to thin, wavy laminations and finely crystalline hematite is present as a

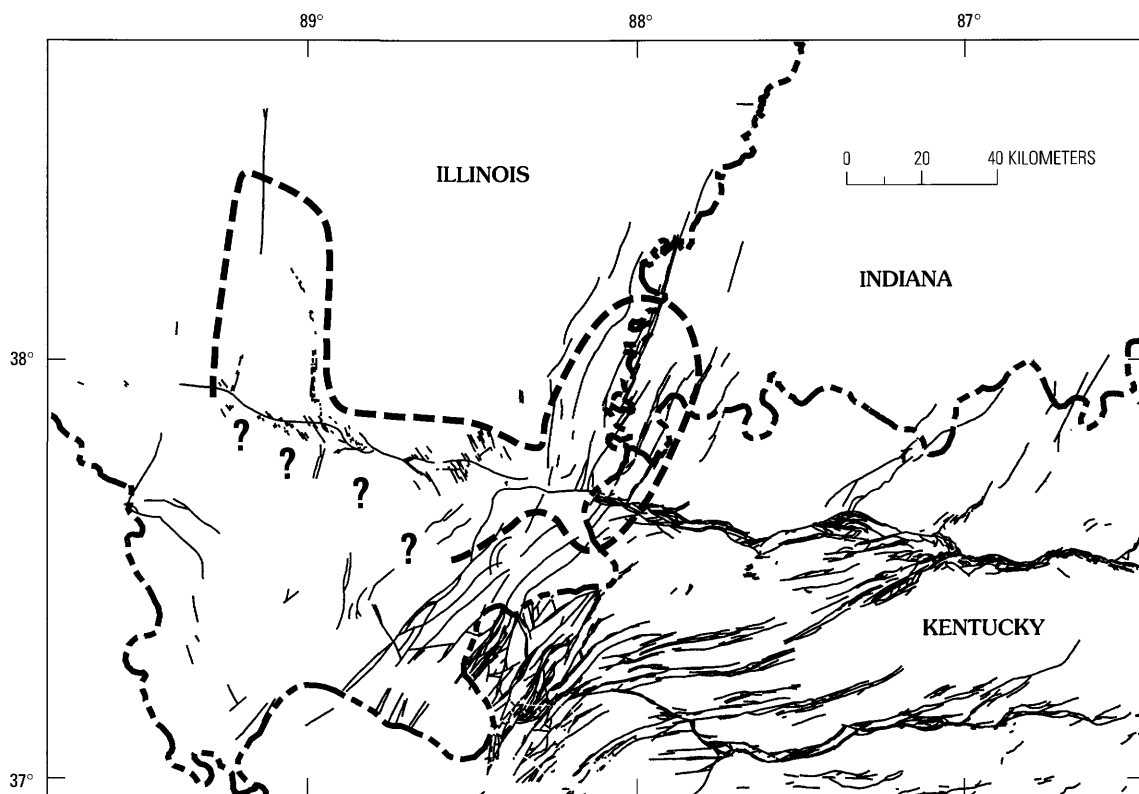


Figure 10. Map showing late-diagenetic quartz and ankerite cementation relative to faults in southern Illinois. Area of cementation defined by dashed line.

dark-red, patchy material in a few sandstones. This distribution of hematite strongly resembles a ferri-argillans mixture of clay minerals and iron oxides/hydroxides as described from soils (cf. Brewer, 1976). A variety of accessory minerals occur in trace amounts.

MINERAL DIAGENESIS

COMPACTION FEATURES

Most sandstones within the Bethel-Cypress interval have undergone some degree of compaction, even in the most porous sandstones. Sandstones that have suffered porosity loss through mechanical compaction did so by means of a gradual increase in grain-packing density as a result of grain rotation and deformation of ductile components. In sandstones that experienced substantial mechanical compaction, there is little or no early cement to provide framework grain support, nor is there evidence of cement-dissolution porosity. Chemical compaction, common in finer grained sandstones, affected quartz grains and early grain overgrowths in contact with early-infiltrated clay. Low amplitude (<5 mm) microstylolites, which account for minor porosity loss, also record the effects of chemical compaction.

SECONDARY QUARTZ

Early diagenetic quartz is the most abundant cement in sandstones (0–23 percent; 7 percent average; table 2) and is widespread throughout the basin. Typically, early authigenic quartz constitutes optically continuous, euhedral overgrowths that are embayed or partially developed. The largest overgrowths are in the coarser grained sandstones. Where early quartz is widespread, it produces well-cemented sandstones that have experienced substantial porosity reduction.

Late-diagenetic(?) quartz is observed in small amounts and is best developed in sandstones close to faults in the southern part of the basin (fig. 10). In thin section, late-stage quartz cement forms coarsely crystalline aggregates that engulf illite, chlorite, and kaolinite and locally coalesce into a clear cement.

CARBONATE CEMENTS

Diagenetic carbonate is common in some sandstones (0–42 percent; 4 percent average; table 2), but in most sandstones it is absent or poorly developed. On the basis of petrographic analysis, early and late stages of carbonate (including syntaxial nonferroan calcite, planar dolospar, poikilotopic ferroan calcite, planar ferroan dolospar

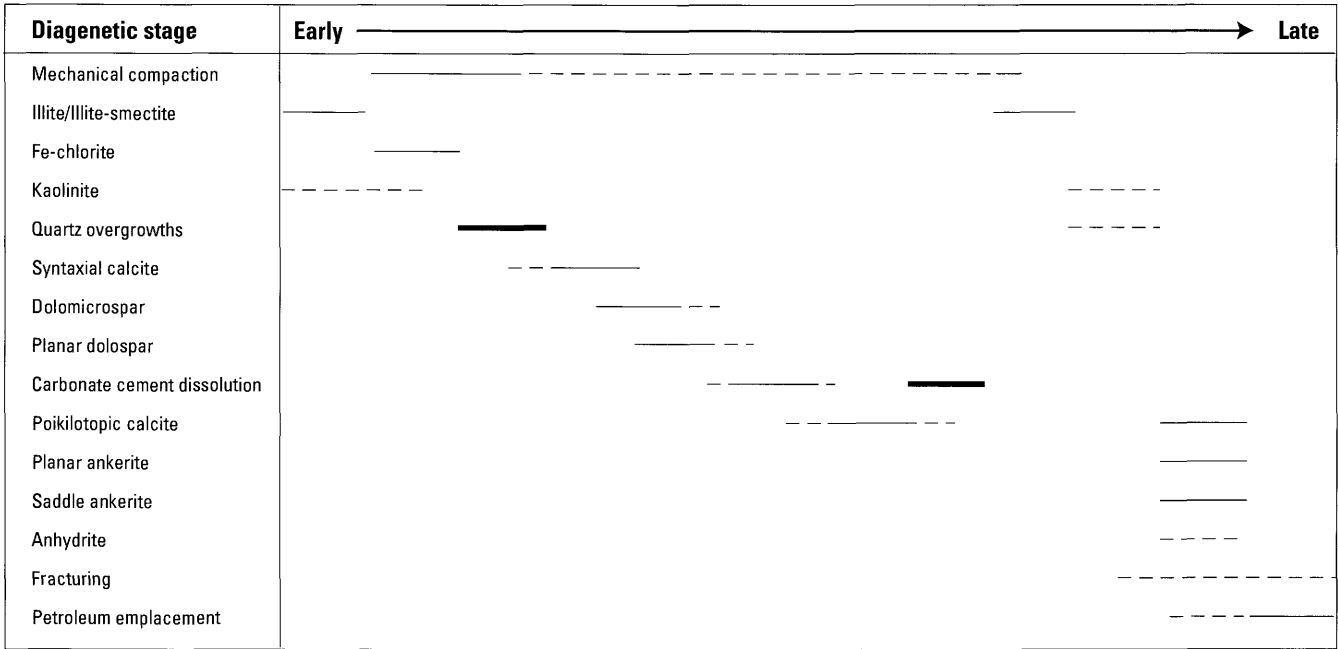


Figure 11. Paragenetic sequence of diagenetic events in reservoir sandstones. Thick bars represent major periods of diagenesis; dashed lines indicate possible diagenesis.

(ankerite), and saddle ankerite) precipitated during the burial history of the Bethel and Cypress Sandstones (see fig. 11). Textural relations between individual phases are complex and often ambiguous, suggesting that there may be additional generations of carbonate that are not recognized. Stable isotope compositions of the major carbonate minerals are reported in table 3 and illustrated in figure 13.

Early- and late-diagenetic carbonates are dominantly pore-fill cements that generally postdate quartz overgrowths. Nonferroan calcite predates other carbonate cements and occurs sporadically in bioclastic sandstones as syntaxial

overgrowths that nucleated on fossil fragments. In some samples, this early calcite has been partially replaced by ferroan calcite cement. The $\delta^{13}\text{C}$ ratio of one sample of syntaxial calcite is -0.12‰ , and the corresponding $\delta^{18}\text{O}$ ratio is -7.80‰ (table 3; fig. 13). Ferroan calcite comprises optically continuous crystals that exhibit straight extinction and, in some sandstones, forms a poikilotopic cement that encloses framework grains. More commonly, ferroan calcite displays poorly defined crystals with irregular grain boundaries and is distributed as relic cement in secondary pores. In a few samples, poikilotopic ferroan calcite partially replaces earlier

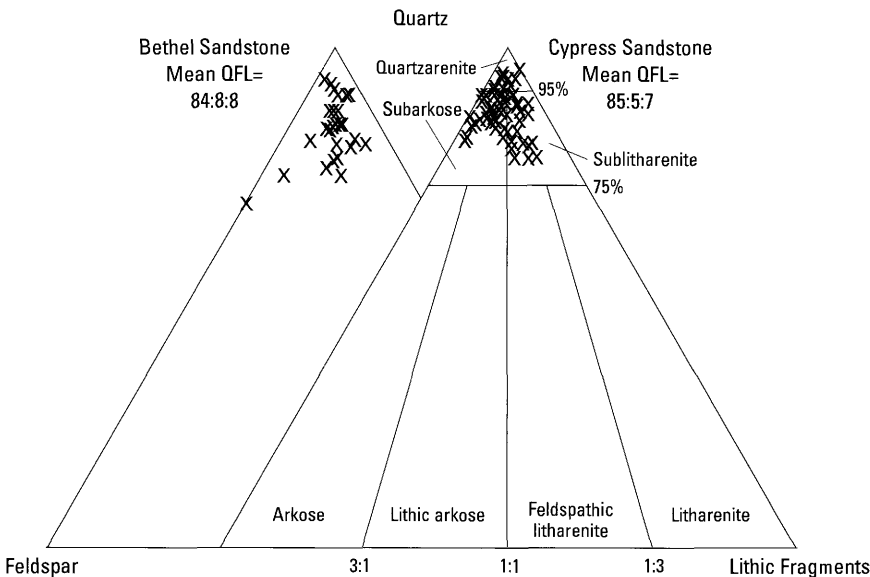


Figure 12. Ternary QFL (quartz, feldspar, lithic fragments) plots for sandstones from the Bethel and Cypress based on the classification of Folk (1974). Note similarity in mineralogic compositions between units.

Table 2. Mineralogic composition of sandstones within the Bethel-Cypress interval.

[Latitude in decimal degrees north; longitude in decimal degrees west. Data reported in volume percent; grain size in micrometers; IGV, intergranular volume; Bi, bimodal]

Core ID	API no.	Latitude	Longitude	Grain size	Quartz size	Na-feldspar	K-feldspar	Total feldspar	Total lithics	Quartz cement	Calcite cement	Dolomite cement	Total carbonate cement	Total cement	Clay	Porosity	IGV
Bethel Sandstone																	
C0071	1207700603	37.928828	89.283433	227	79	1	0	1	4	3	0	0	0	4	0	12	12
C0285	1214502037	38.158661	89.285138	152	64	1	4	5	7	4	0	0	0	4	0	17	21
C0318	1216501136	37.878645	88.578628	69	52	5	2	7	9	15	0	12	12	27	0	2	29
C0345	1208102322	38.320668	89.042866	152	65	1	3	4	5	6	18	1	19	25	0	8	33
C0361	1204700033	38.481371	88.014630	190	58	4	0	4	4	6	2	0	2	16	8	14	30
C0364	1202702511	38.518618	89.424022	265	67	4	1	5	2	3	2	4	6	9	0	15	24
C0414	1202900030	39.595217	88.388347	303	50	0	0	0	22	1	22	3	25	26	0	0	26
C0467	1219304604	38.160159	87.986364	190	49	5	2	7	7	1	0	0	0	1	0	4	5
C0468	1219306807	37.929945	88.285574	190	60	5	6	11	9	9	0	0	1	10	1	8	18
C0518	1202700823	38.658891	89.278940	127	69	5	2	7	5	0	0	0	0	5	5	9	14
C0525	1200500212	38.978035	89.309814	152	40	1	2	3	1	0	0	1	1	1	0	7	8
C0573	1202500986	38.772606	88.753333	190	65	2	3	5	4	6	0	0	0	6	0	16	22
C0595	1204900704	38.958267	88.624839	Bi	69	3	1	4	3	7	0	0	0	13	6	10	23
C0597	1207900017	38.878071	88.352995	152	68	2	4.5	6.5	5.5	5	1	0	1	6	0	6.5	12.5
C0607	1205500336	37.867485	88.975637	190	61	7	0	7	6	4	2	4	6	17	7	4	21
C0651	1218900150	38.252045	89.403828	114	60.5	0.5	7	7.5	6.5	4.5	0	0	0	4.5	0	17	21.5
C0735	1212101296	38.705799	89.055451	303	66	1	1	2	3	9	4	0	4	13	0	15	28
C1018	1212104149	38.561675	89.020984	152	59	3	5.5	8.5	7.5	3.5	3	0	3	8	1.5	12	20
C1113	1218900176	38.470347	89.210327	265	69	2	1	3	3	5	1	0	1	6	0	19	25
C1125	1212590017	38.772307	88.073440	152	68	1	3	4	11	6	0	0	0	6	0	2	8
C1169	1217300051	39.326445	88.906719	152	54	2	3	5	6	9	1	1	2	11	0	22	33
C1270	1208100499	38.405546	88.831430	265	58	5	4	9	5	15	4	0	4	20	1	8	28
C1511	1204900140	39.065321	88.765539	190	61	2	3	5	5	9	5	0	5	17	3	11	28
C2069	1212101475	38.778051	88.762495	152	58	1	4	5	6	14	3	0	3	22	5	10	32
C2085	1212104968	38.779868	88.755532	152	49	2	2	4	4	0	36	3	39	39	0	1	40
C2114	1202500549	38.710497	88.584495	114	66	1	5	6	6	8	1	0	1	14	5	8	22
C2230	1200500567	38.827081	89.474212	114	60	6	3	9	4	4	0	0	0	11	7	15	26
C2341	1208100199	38.181586	88.992598	190	59	3	4.5	7	7	5.5	1	1	2	8	0.5	6.5	14.5
IN303	no data	38.185565	86.508559	190	53	3	2	5	6	11	0	12	12	24	1	1	25
IN643	no data	38.345879	86.704695	152	39	0	2	2	11	0	0	1	1	1	0	0	1

Table 2. Mineralogic composition of sandstones within the Bethel-Cypress interval—Continued.

Core ID	API no.	Latitude	Longitude	Grain size	Quartz	Na-feldspar	K-feldspar	Total feldspar	Total lithics	Quartz cement	Calcite cement	Dolomite cement	Total carbonate cement	Total cement	Clay	Porosity	IGV
Cypress Sandstone																	
C00071	1207700603	37.928828	89.283433	190	68	3	0	3	1	9	0	0	0	10	1	17	27
C00285	1214502037	38.158661	89.285138	152	61	6	1	7	2	4	1	4	5	9	1	16	25
C00374	1219901289	37.820457	88.825271	303	49	5	0	5	1	2	0	38	38	41	1	0	41
C00385	1215900044	38.725340	88.185230	152	70	1	0	1	3	12	11	0	11	23	0	2	25
C00467	1219304604	38.160159	87.986364	152	55	11	0	4	6	6	0	0	0	10	4	17	27
C00491	1205500563	38.029849	88.946832	190	63	5	0	5	3	6	0	0	0	9	3	17	26
C00520	1204700028	38.481310	87.999950	265	50	0.5	0.5	1	9.5	5	22.5	3	25.5	32	1.5	6.5	38.5
C00592	1219300424	38.153027	88.043539	190	57.5	8	0	5.5	2.5	5.5	0	0	0	12.5	7	16.5	29
C00597	1207900017	38.878071	88.352995	265	61	7.5	0	7.5	2	8.5	0	1	1	10	0.5	17	27
C00642	1206502267	38.006169	88.605524	152	54	3	0	3	6	15	0	7	7	25	3	7	32
C00671	1205500350	38.085232	88.760615	190	59	1	0	1	2	12	0	2	2	16	2	18	34
C00693	1205500244	37.922344	88.939580	379	72.5	1.5	0	1.5	2.5	2.5	7.5	0	7.5	11.5	1.5	10	21.5
C00735	1212101296	38.705799	89.055451	190	54.5	6	3.5	10	5	6.5	0	0	0	9.5	3	13.5	23
C00962	1216502428	37.661006	88.539391	152	57	1	0	1	4	16	0	5	5	33	12	0	33
C00996	1219105483	38.588268	88.322813	227	58	7	2	9	7	19	0	0	0	20	1	5	25
C01049	1213900006	39.581258	88.534095	190	58	3	0	3	7	12	0	1	1	13	0	17	30
C01096	1202700576	38.65244	89.198733	114	61	8	1	9	5	3	0	0	0	10	7	4	14
C01103	1218900387	38.277920	89.247419	190	64	3	0	3	2	11	1	1	2	15	2	15	30
C01113	1218900176	38.470347	89.210327	190	61	3	0	3	3.5	10	0	2	2	12	0	19	31
C01135	1207900014	39.164720	88.233602	303	63	3	0	3	3	10	1	7	8	20	2	9	29
C01160	1208100552	38.282282	88.908279	76	69	2	0	2	4	3	0	0	0	15	12	2	17
C01183	1219306873	37.926202	88.278548	190	65	4	0	4	4	7	0	0	0	9	2	17	26
C01309	1218500599	38.496459	87.780426	114	61	6	0	6	6	8	0	0	0	11	3	11	22
C01353	1204700182	38.398650	87.983098	152	59	5	0	5	6	9	0	1	1	13	3	14	27
C01439	1208100764	38.263679	89.085271	341	67	5	0	5	1	12	0	0	0	13	1	12	25
C01445	1219101791	38.589686	88.279198	190	59	8	0	8	5	4.5	0	0	0	6.5	2	10	16.5
C01511	1204900140	39.065321	88.765539	190	57.5	5.5	4	9.5	3.5	5.5	1	0.5	1.5	8.5	1.5	18.5	27
C01546	1202500525	38.789958	88.419539	227	60.5	6	0.5	6.5	3.5	6.5	0	0	0	8	1.5	18	26
C01558	1202901169	39.469611	88.379941	114	53	1	0	1	8	9	5	8	13	26	4	2	28
C01698	1202900325	39.460276	88.396417	190	60	2	0	2	5	8	1	0	1	9	0	24	33
C01704	1202900291	39.420342	88.376784	102	61	1	0	1	10	0	0	0	0	0	0	20	20
C01717	1202901131	39.463975	88.403436	152	63	0	3	3	6	3	5	0	5	8	0	21	29
C01735	1202901134	39.474788	88.400756	114	60	0	0	0	6	5	0	0	0	14	9	20	34
C01740	1202901301	39.433612	88.398575	152	64	0.5	1	1.5	5	2	5.5	0.5	6	8.5	0.5	18.5	27

Table 2. Mineralogic composition of sandstones within the Bethel-Cypress interval—Continued.

Core ID	API no.	Latitude	Longitude	Grain size	Quartz	Na-feldspar	K-feldspar	Total feldspar	Total lithics	Quartz cement	Calcite cement	Dolomite cement	Total carbonate cement	Total cement	Clay	Porosity	IGV
C01760	1202900795	39.427991	88.393260	114	65	0	0	0	10	3	1	0	1	4	0	14	18
C01794	1202901319	39.437038	88.386898	152	60.5	2.5	0	2.5	3.5	6	0.5	0	0.5	6.5	0	19	25.5
C01806	1202900869	39.414467	88.395643	190	57	0	2	2	7	5	0	0	0	8	3	7	15
C01813	1203500074	39.337077	88.433253	114	53	5	2	7	6	23	2	0	2	29	4	0	29
C01834	1202901353	39.442305	88.377306	152	60	0.5	0	0.5	6.5	5	0.5	0	0.5	10.5	5	20	30.5
C01931	1202901019	39.502063	88.398420	152	57	1.5	0	1.5	4.5	4.5	0	0	0	8	3.5	25	33
C01968	1202901330	39.433810	88.380040	152	50	0	1	1	10	1	35	0	35	36	0	0	36
C01975	1202900788	39.424176	88.386237	190	65	0	0	0.5	6	5	1	0	1	6	0	17.5	23.5
C01981	1207900301	38.881033	88.230995	152	59	4	0	4	7	11	0	0	0	14	3	12	26
C02114	1202500549	38.710497	88.584495	227	52	4	1	5	6	12	0	0	0	16	4	19	35
C02149	1219101213	38.435874	88.278806	227	67	3	0	3	2	16	0	0	0	20	4	5	25
C02174	1204900813	38.946928	88.480065	190	67	4	0	4	5	8	1	0	1	12	3	10	22
C02230	1206500567	38.827081	89.474212	190	61.5	4	1	5	2.5	2	3	0	3	7	2	22	29
C02357	1212101986	38.765089	88.902172	190	58	2	0	2	4	20	5	7	12	32	0	3	35
C02621	1205901062	37.704520	88.173993	190	55	7	2	9	4	18	0	5	5	26	3	2	28
C05279	1218502475	38.260543	87.944239	265	68	2.5	0	1.5	2.5	3	0	0	0	5.5	2.5	19.5	25
C05834	1202501165	38.627951	88.610797	190	70	0	2	2	8	5	0	0	0	5	0	15	20
C05874	1218900972	38.233049	89.690740	152	52	5	1	6	4	5	0	7.5	7.5	14.5	2	21	35.5
C06058	1219302857	38.053129	88.174550	227	60	5	0	5	6	12	0	6	6	22	4	0	22
C06079	1203307971	38.867555	87.788940	152	58.5	5	2	7	6	5	2	0.5	2.5	9	1.5	16.5	25.5
C14018	1210127623	38.753134	87.783338	114	44	1	0	1	6	0	40	2	42	42	0	5	47
C14019	1210128363	38.759770	87.786930	114	62	1	0	1	4	2	26	0	26	28	0	4	32
C14023	1204724183	38.562076	88.025117	114	67	2	0	2	2	5	1	0	1	9	3	4	13
IN071	no data	38.086299	87.381803	190	61	1	2	3	5	1	1	3	4	5	0	14	19
IN097	no data	38.681153	86.687115	190	63	0.5	2.5	3	3	11	0	0	0	18	3.5	14.5	32.5
IN133	no data	38.238589	87.932857	190	61.5	3	0	3	6.5	3.5	0	2.5	2.5	6	0	17	23
IN643	no data	38.345879	86.704695	152	48.5	0.5	3	3.5	5	0.5	0	30.5	30.5	31	0	10	41
IN647	no data	38.330681	87.655480	152	70	2	0	2	7	0	0	0	0	0	0	20	20
IN734B1	no data	38.511973	87.418606	227	70	1	3	4	6	1	6	0	6	7	0	10	17
IN745	no data	39.062193	86.857040	152	69	0	4	4	5	1.5	0	0	0	6.5	5	18	24.5

Table 3. Stable isotope compositions of carbonate cements in sandstones within the Bethel-Cypress interval.[Values in parentheses are repeated analyses. $\delta^{13}\text{C}$ and $\delta^{18}\text{O}$ values in per mill, PDB]

Sample ID	Depth (m)	Unit	$\delta^{13}\text{C}$	$\delta^{18}\text{O}$
Syntaxial calcite				
C00414	1,785	Bethel	-0.12	-7.80
IN734	1,392	Cypress	-19.39 (-19.43)?	-8.63 (-8.68)
Poikilotopic Fe-calcite				
C00345	2,025	Bethel	-5.60	-10.5
C00345	2,020	Bethel	-3.09	-9.90
C01270	2,662	Bethel	-2.55	-9.50
C00385	2,859	Cypress	-2.59 (-2.59)	-10.35 (-10.35)
C00520	2,859	Cypress	-2.71 (-2.71)	-8.76 (-8.76)
C00693	2,471	Cypress	-15.83 (-15.75)	-8.70
C01301	1,787	Cypress	-11.27 (-11.19)	-9.71 (-9.93)
C01698	1,756	Cypress	-1.97 (-2.01)	-11.30 (-11.20)
C01968	1,901	Cypress	-2.14 (-2.23)	-10.70 (-10.90)
C01975	1,880	Cypress	-2.17 (-2.35)	-10.80 (-10.50)
C01975	1,880	Cypress	-2.27 (-2.27)	-10.56 (-10.62)
C08363	1,311	Cypress	-4.22 (-4.22)	-7.92 (-7.92)
C14019	1,311	Cypress	-4.26	-7.80
Planar ankerite				
C00071	1,655	Bethel	-1.97	-7.40
C00318	2,972	Bethel	-2.81	-6.60
C00607	2,557	Bethel	-1.52	-7.70
IN303	538.5	Bethel	-0.64	-6.60
C00642	2,822	Cypress	-0.56	-6.60
C00962	2,009	Cypress	0.02	-9.00
C05874	819	Cypress	-0.26	-5.60
C05874	817	Cypress	-0.34	-5.80
IN643	422	Cypress	1.65	-5.00
IN643	440	Cypress	0.32 (0.32)	-5.56 (-5.56)
Saddle ankerite				
C00285	1,157	Cypress	-3.33	-11.80
C00374	2,584	Cypress	-8.85	-9.60
C01183	2,584	Cypress	-5.38	-7.40
C01353	2,717	Cypress	-2.63	-7.5
C01981	2,752	Cypress	-4.04	-8.20
IN71	1,672	Cypress	-2.68 (-2.61)	-7.39 (7.18)

formed syntaxial calcite and is in contact with early quartz overgrowths. It also occurs locally as a late-stage fracture-fill cement that crosscuts earlier carbonate and quartz overgrowth cements. The $\delta^{13}\text{C}$ values of poikilotopic ferroan calcite cluster in two groups; most samples display slightly negative $\delta^{13}\text{C}$ values ranging from -1.97 to -5.60‰ , but two samples yielded highly negative $\delta^{13}\text{C}$ values of -11.27 and -15.83‰ . $\delta^{18}\text{O}$ values of ferroan calcite samples vary from

-7.80 to -11.30‰ (table 3; fig. 13). A small component of dolomite in sandstones is classified as early, nonferroan, planar dolospar on the basis of its straight crystal boundaries and even extinction in polarized light. Most planar dolospar is compositionally homogeneous, but some dolospar grains exhibit well-developed Fe-rich overgrowths and are zoned. Except for its relationship with ankerite, the paragenesis of planar dolospar is ambiguous because it rarely occurs with

other carbonate cements. Unfortunately, planar dolospar is present in small amounts, or as complex intergrowths with ankerite, and thus could not be sampled for isotopic analysis.

Late-diagenetic planar ankerite postdates early carbonate cements and predates hydrocarbon emplacement in reservoir sandstones. Planar ankerite typically occurs as solitary or clustered rhombs, and where abundant, forms irregular, coarsely crystalline or monocrystalline cement that infills secondary voids and replaces feldspar grains. Nowhere does it show evidence of dissolution. In some sandstones, a component of ankerite is anhedral to subhedral in habit with slightly to moderately curved crystal faces and broad sweeping extinction—features that classify it as saddle ankerite. This type of ankerite occurs as a pore-fill cement and fills fractures that crosscut earlier formed quartz and carbonate cements. Saddle ankerite (and planar ankerite) are most abundant in sandstones close to faults in the southern part of the basin (fig. 10). The isotope ratios of planar ankerite vary over a relatively narrow range, from 1.65 to -2.81‰ ($\delta^{13}\text{C}$) and -5.00 to -7.70‰ ($\delta^{18}\text{O}$), and are consistently heavier than the ratios of saddle ankerite, which range from -2.63 to -8.85‰ ($\delta^{13}\text{C}$) and -7.39 to -11.80‰ ($\delta^{18}\text{O}$) (table 3; fig. 13).

AUTHIGENIC CLAY MINERALS

Minor authigenic clay (0–7 percent, average 2 percent; table 2) is observed in most sandstones within the Bethel-Cypress interval. Illite and randomly ordered, interstratified illite/smectite are present as both precompaction and post-compaction clay. Precompaction (syndepositional) illite consists of thin tangential coatings on framework quartz grains devoid of authigenic overgrowths in finer grained sandstones. Where grain-rimming illite is widespread, quartz grains commonly display interdigitated, presolved contacts. Postcompaction illite is distributed as wispy, irregular flakes on detrital grains and, less commonly, as pore-bridging and pore-filling aggregates. Petrographic analysis suggests there are at least two stages of this later illite. The earlier phase is intergrown with authigenic quartz overgrowths, whereas a later phase is associated with residual pores and leached potassium-feldspar grains.

Other diagenetic clays in sandstones include Fe-rich chlorite and kaolinite. Authigenic chlorite occurs as euhedral platelets (1–5 μm in diameter) that form tangential rims on framework grains, principally detrital quartz devoid of authigenic overgrowths. The chlorite rims commonly are discontinuous and bridge framework grains at grain contacts. Kaolinite forms small (2–5 μm), randomly oriented, pseudohexagonal platelets and loosely to densely packed aggregates of platelets that line and infill secondary pores. In rare instances, it replaces partially dissolved feldspar grains. Kaolinite is most abundant near the basin margin where Chesterian-age sandstones were affected by subaerial erosion, but in southern Illinois, rare dickite, a high-temperature kaolin polymorph, occurs locally.

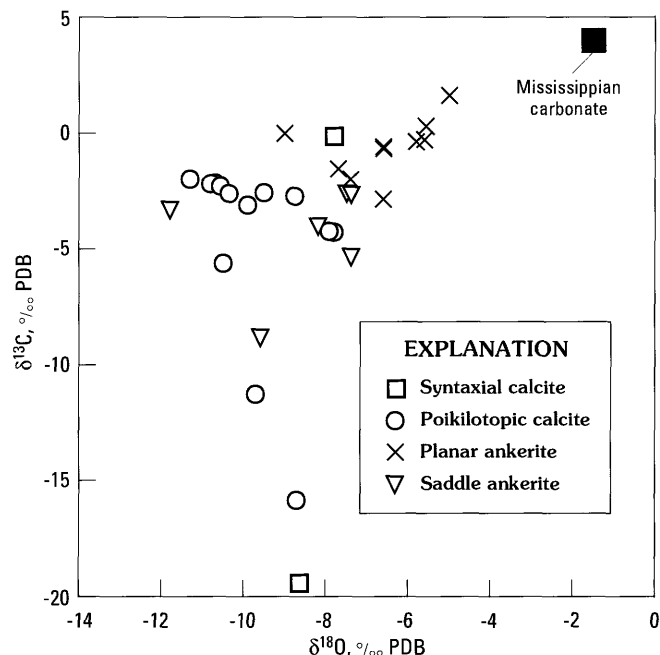


Figure 13. Stable isotope compositions of diagenetic carbonate cements in reservoir sandstones. Black square represents approximate composition of carbonate cement in equilibrium with Mississippian seawater (from Meyers and Lohmann, 1985). Note substantial overlap between the different carbonate types. PDB, Peedee belemnite standard.

OTHER PHASES

Anhydrite is present in volumetrically minor amounts in a few samples of Cypress Sandstone. Its mode of occurrence ranges from small scattered patches to large euhedral crystals that preferentially replace ferroan calcite and fill secondary(?) pores. There is no evidence to suggest that anhydrite was affected by dissolution processes.

Pyrobitumen is present locally as an opaque residue in some sandstones within the Bethel-Cypress interval. Within oil zones, pyrobitumen occupies moldic and intergranular (secondary) pores and, in a few samples, rims planar ankerite cement. Petroleum residue in sandstones also is observed coating minor quartz overgrowths and relic ferroan and non-ferroan calcite cement.

Other authigenic phases in insignificant amounts include pyrite, siderite, and barite.

SECONDARY POROSITY

Secondary porosity occurs at all depths and was produced by the dissolution of carbonate cement, principally nonferroan and ferroan calcite, and framework grains. Removal of calcite ranges from minor corrosion to complete dissolution. In sandstones where calcite has been

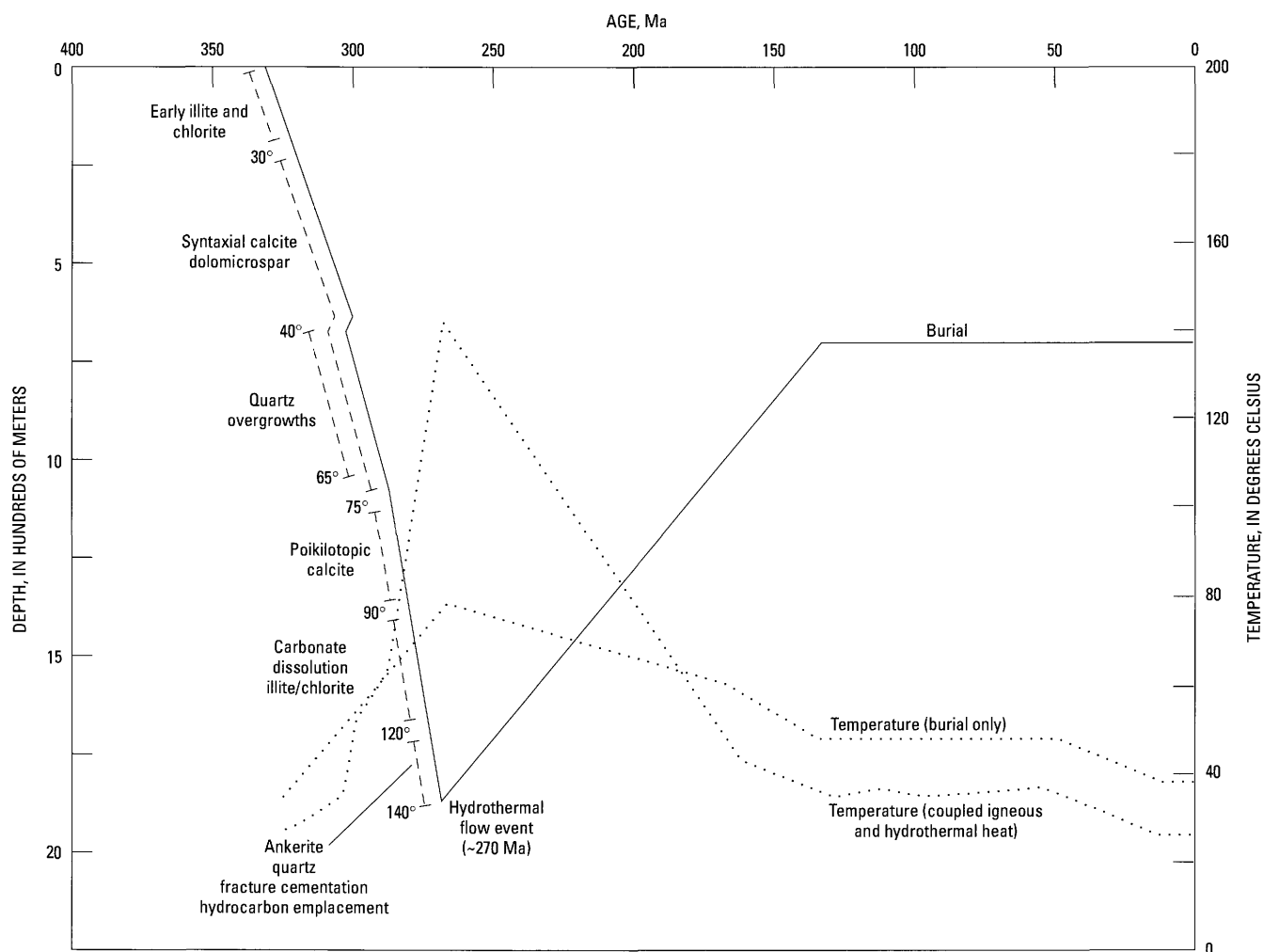


Figure 14. Burial and thermal history curves for the Bethel Sandstone–Cypress Sandstone interval showing relative timing of major diagenetic events in southern and central Illinois. Age of fluorite and petrographic features constrain the timing of diagenesis; age of regional hydrothermal fluid-flow event (~270 Ma) is shown for comparison. Paleotemperature profiles (igneous plus hydrothermal heat flow and burial only heat flow) were determined using a coupled fluid-flow and burial heat-flow model. The temperatures bracketing diagenetic events were modified from Surdam and others (1989). Note that thermal curves are depicted relative to geologic age rather than burial depth.

dissolved, quartz grains have irregular embayments and overgrowths display partially developed or embayed boundaries. The size and shape of grain and overgrowth reentrants combined with relic calcite replacing framework grains attest to the dissolution of preexisting calcite cements. Additional lines of evidence in favor of calcite-cement dissolution include well-developed intergranular calcite cement immediately adjacent to extensively leached areas and scattered dissolution voids in tightly cemented sandstones. Leaching of framework grains affected mainly detrital alkali feldspars and resulted in the formation of oversized and moldic pores. In some sandstones, there is no clear evidence that leaching was due to the dissolution of replacement carbonate. Overall, grain-dissolution porosity

typically is less than a few percent and did not substantially enhance the total sandstone porosity.

In moderately to highly porous sandstone, framework-grain-supporting cements clearly were removed, but all intergranular porosity may not have resulted from dissolution processes. If initial cementation was incomplete, some primary porosity should be preserved in reservoir sandstones. Distinguishing primary from secondary porosity proved to be difficult; thus, estimated amounts of primary porosity are not reported. Nevertheless, textural features together with heterogeneous grain-packing densities suggest that the intergranular pore system in sandstones is predominantly secondary with only minor primary porosity preserved locally.

EVOLUTION OF RESERVOIR QUALITY

The evolution of the diagenetic system in the Bethel and Cypress Sandstones in central and southern Illinois is shown on a reconstructed burial curve in figure 14. Major diagenetic events include (1) precompaction (syndepositional) illite and early chlorite precipitation; (2) quartz, calcite, and dolospar cementation; (3) calcite cement and framework grain dissolution; (4) illite and kaolinite formation; (5) late quartz and ankerite precipitation; (6) fracture cementation; and (7) hydrocarbon emplacement. The temperatures that correspond to individual diagenetic phases were modified from Surdam and others (1989) and correlated with the temperature profile that is based on the combined thermal effects of igneous heat and hydrothermal fluid flow (fig. 14). A temperature curve derived on the basis of burial heat flow alone is shown for comparison.

Late-diagenetic fluorite, containing oil-bearing fluid inclusions, in the Illinois/Kentucky Fluorspar district has been dated at ~270 Ma (Richardson and others, 1988; Chesley and others, 1994). Although Upper Mississippian sandstones lack cements suitable for isotopic age dating and individual diagenetic events have no specific time connotation beyond "early" and "late," the timing of peak hydrocarbon migration in the basin (~270 Ma) places an upper limit on the age of much of the diagenesis in reservoir sandstones. The steep trend of the burial curve (fig. 14) indicates that diagenesis in sandstones occurred over a short geologic time interval (<~60 m.y.) and was largely complete by the time the rocks had reached their maximum burial in the late Paleozoic.

QUARTZ CEMENTATION

On the basis of burial-thermal modeling, most quartz cement that precipitated early in the burial history formed at relatively low temperatures (<~65°C), but minor late-diagenetic quartz in sandstones near faults in the southern part of the basin may have precipitated from fluids with temperatures as high as ~140°C (fig. 14). Feldspar leaching probably was not a major source of silica for early quartz overgrowth development because framework grain dissolution occurred after most quartz precipitation had ended. Pressure solution along stylolites and on grain contacts often is cited as an important source of silica for quartz cementation in sandstones (Bjorlykke and Egeberg, 1993; Houseknecht, 1984, 1988). Petrographic analysis shows evidence for incipient stylolitization and grain-to-grain contact dissolution in some sandstones within the Bethel, but the amount of silica released is difficult to determine directly because stylolite amplitudes and overlap quartz cannot be easily measured. In thin section, framework grain contacts and microstylolite seams commonly contain illitic clay. Studies by Heald (1955) and Weyl (1959)

demonstrated that, although pressure solution may occur without clay, clay coatings accelerate the grain-to-grain contact-dissolution process. Silica-rich pore fluids produced by pressure solution at stylolites or at grain contacts subsequently diffuse over relatively short distances to sites of quartz precipitation. Several studies have argued that the transformation of smectite to illite in interstratified clays is a potential silica source for quartz cementation (Siever, 1962; Hower and others, 1976; Boles and Franks, 1979). Mixed-layer illite/smectite is minor in shallowly buried sandstones within the Bethel-Cypress interval, and shale interbeds containing mixed-layer clay generally are sparse; thus, the illite/smectite transformation process probably did not contribute a significant amount of silica for early quartz cement. Much of the silica for early quartz cementation might have originated from extrastratal sources, including saturated meteoric ground waters that circulated through the sandstones following deposition. In southern Illinois, a component of silica incorporated into late-stage quartz may have been derived from an igneous source.

CARBONATE DIAGENESIS

Carbonate cementation in sandstones began soon after early quartz precipitation and continued until the emplacement of hydrocarbons (fig. 14). Overall, carbonate cements become more coarsely crystalline, enriched in Fe, depleted in ^{18}O , and confined to preexisting intergranular porosity with increasing diagenesis. These phenomena have been noted in other sedimentary basins and have been attributed to precipitation from low-Eh pore waters under gradually increasing burial temperatures. In the Illinois Basin, increasing temperature with time records the increased effects of heat related to igneous activity and fluid flow in addition to burial. Most carbonate cements in sandstones within the Bethel-Cypress interval have slightly negative $\delta^{13}\text{C}$ values (-3‰ average), indicating a strong influence from a marine carbon source (i.e., carbonate fossils and chemically unstable calcite cement). The restricted range in carbon-isotope compositions suggests that the carbonate system was controlled largely by the conditions that existed during initial carbonate precipitation, modified later by water-rock interaction. It is important to note that the marine carbon signature in carbonate cements has been preserved even when the $\delta^{18}\text{O}$ values reflect reequilibration, consistent with petrographic observations showing carbonate recrystallization. A few calcite samples in southern Illinois are depleted in ^{13}C with respect to inorganic carbon and have compositions of -11 to -16‰ (see table 3 and fig. 13). These light values are unusual for the Bethel and Cypress and probably reflect a contribution of light carbon from decarboxylized organic matter in a system buffered by marine carbon. Between 10 and 50 percent of the organic carbon introduced into the diagenetic system must have had a $\delta^{13}\text{C}$ of -26‰ in order to explain these light

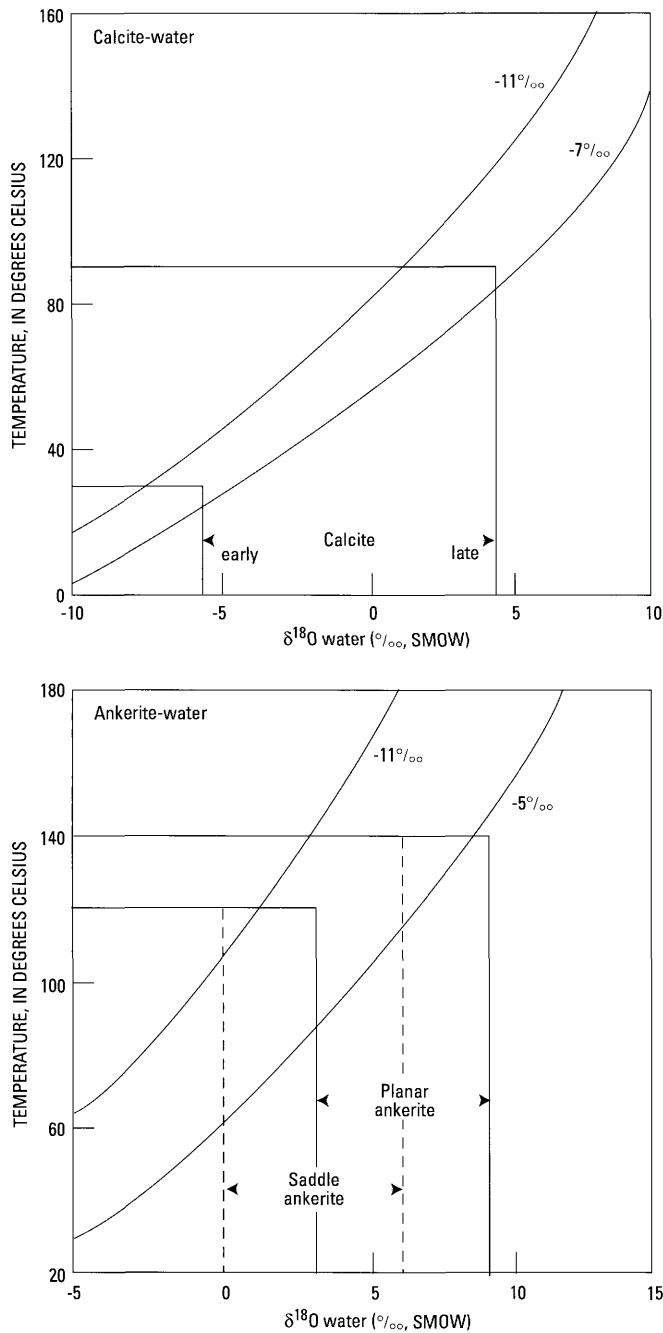


Figure 15. Equilibrium relationship between $\delta^{18}\text{O}$ of water, $\delta^{18}\text{O}$ of calcite and ankerite, and crystallization temperature. Curves represent locus of temperature and possible $\delta^{18}\text{O}$ of water in equilibrium with a mineral having the indicated oxygen isotopic composition. Fractionation equations (calcite-water: $10^3 \ln \alpha = 2.78 \times 10^6 \times T^{-2} - 2.89$ and ankerite-water: $10^3 \ln \alpha = 2.78 \times 10^6 \times T^{-2} + 0.11$) are from Friedman and O'Neil (1977) and Fritz and Smith (1970), respectively. SMOW, Standard mean ocean water.

values. In the southern part of the basin, $\delta^{13}\text{C}$ values of saddle ankerite are slightly depleted relative to the $\delta^{13}\text{C}$ values of planar ankerite cement. The $\delta^{13}\text{C}$ values of saddle ankerite generally are within the range of marine values,

indicating that the carbon-isotope composition of the fluid from which the saddle ankerite precipitated was largely controlled by the carbon composition of the host sandstones.

The oxygen isotopic composition of carbonate cements in sandstones varies over a wide range (~ -5 to -12‰) and, as will be shown, was controlled by the isotopic composition of the precipitating fluids and the temperature of crystallization. By knowing the oxygen-isotope compositions of calcite and dolomite cement, the isotopic composition of carbonate-precipitating waters can be reconstructed by calculating equilibrium $\delta^{18}\text{O}_{\text{H}_2\text{O}}$ values, based on estimated temperatures of crystallization (fig. 15). Two assumptions are pertinent to this approach: the carbonate minerals formed in isotopic equilibrium with the pore waters and no temperature inversions occurred from the time of initial burial through ankerite precipitation. In making $\delta^{18}\text{O}_{\text{H}_2\text{O}}$ calculations, we used the fractionation equation of Friedman and O'Neil (1977) for calcite and Fritz and Smith (1970) for dolomite. Precipitation temperatures of carbonate cements cannot be constrained directly because no fluid inclusions were found in individual carbonate minerals; therefore, estimated carbonate precipitation temperatures were taken from the burial-thermal profiles in figure 14. It is noteworthy that carbonate-precipitating temperatures at shallower depths of burial ($< \sim 1,000$ m) were governed by burial (conductive) heat flow, whereas, at greater depths of burial ($> \sim 1,000$ m), temperatures of crystallization were influenced by advective heat from hydrothermal fluids.

Using a near-surface temperature of $\sim 30^\circ\text{C}$, early syntaxial calcite precipitated from waters with oxygen-isotope compositions of $\sim -6\text{‰}$ SMOW (standard mean ocean water) (fig. 15). Presumably, early dolomicrospar formed from similar waters at about the same temperatures. The negative oxygen isotope ratios of early calcite (and dolomite) relative to Mississippian marine carbonate (see fig. 13) indicate that the initial diagenetic environment was fresh-water influenced, if not fresh-water dominated, during precipitation of the earliest carbonate cements. Poikilotopic ferroan calcite postdates quartz overgrowths and early syntaxial calcite but predates hydrocarbon emplacement; thus it conceivably formed at a temperature as high as $\sim 90^\circ\text{C}$ (Surdam and others, 1989). Estimated pore-water compositions at these temperatures vary from ~ 0 to 4‰ SMOW (fig. 15). Planar ankerite is a late-diagenetic carbonate phase that formed just prior to hydrocarbon emplacement when the host sandstones were close to their maximum depth (~ 2 km). The iron enrichment of planar ankerite (and ferroan calcite) is consistent with precipitation from Fe-enriched reducing waters, and the light $\delta^{18}\text{O}$ isotope values indicate precipitation at elevated temperatures. Assuming an estimated formation temperature of $\sim 120^\circ\text{--}140^\circ\text{C}$, planar ankerite precipitated from ^{18}O -enriched waters with compositions ranging from ~ 3 to 9‰ SMOW (fig. 15). Saddle ankerite commonly is associated with fractures in the southern portion of the basin (fig. 10) and postdates all other mineral cements in sandstones.

Assuming minimum temperatures on the order of 120°C, $\delta^{18}\text{O}_{\text{H}_2\text{O}}$ values of ~ 0 to 5‰ SMOW are estimated, and slightly heavier values, ~ 6 ‰ SMOW, are plausible if fluids with temperatures as high as 140°C were involved in saddle ankerite cementation.

CLAY MINERAL PRECIPITATION

Clay mineral authigenesis began before significant compaction and continued until late in the burial history (fig. 14). Illite rims that predate mechanical compaction and underlie quartz overgrowths are regarded as a syndepositional or very early diagenetic precipitate. Postcompactional illite occludes some secondary pores, indicating it postdated carbonate dissolution but predated hydrocarbon emplacement. Postcompactional illite associated with leached detrital potassium feldspar grains indicates a genetic link between feldspar dissolution and illite that replaces feldspar. The illitization of smectite likely reflects increasing temperature, either as a consequence of burial or due to the introduction of an additional source of heat to the sediments late in the burial history.

The chlorite rims on framework grains are discontinuous and, in some sandstones, bridge framework grain contacts, indicating some mechanical compaction had occurred prior to chlorite precipitation. The relationship between Fe-rich chlorite and quartz overgrowths is ambiguous, but the lack of early quartz overgrowths on grains rimmed with authigenic chlorite suggests that the formation of chlorite inhibited quartz cementation. Iron-oxide grain coatings and dewatering of shales were potential sources of iron incorporated into chlorite.

Textural evidence is conflicting relative to the timing of kaolinite precipitation. Kaolinite is observed in dissolution(?) pores in shallowly buried sandstones, suggesting that it postdated calcite precipitation. Hydrocarbon emplacement followed carbonate dissolution and the formation of kaolinite, which indicates that kaolinite was not the most recent diagenetic event and thus precipitated at temperatures below the estimated maximum of 140°C. Kaolinite forms at low pH when there is an excess of silica and few K and Mg ions in solution, conditions that occurred during several periods of diagenesis. Assuming formation under these conditions, kaolinite could have precipitated during early diagenesis by ground waters entering sandstones at the post-Mississippian unconformity underlying Pennsylvanian strata, or it may have formed later as a consequence of meteoric diagenesis associated with late Paleozoic uplift and erosion. In south-central Illinois, away from meteoric water invasion, minor kaolinite at moderate burial depths may reflect SiO_2 and Al_2O_3 released into solution via pressure solution of quartz and decomposition of feldspar. On the southern tectonic flank of the basin, transformation of kaolinite to dickite probably occurred in response to the influx of high-temperature fluids into reservoir sandstones.

SECONDARY POROSITY DEVELOPMENT

Detailed petrographic evidence summarized above indicates that dissolution of carbonate cement (mostly calcite) and selective leaching of feldspar grains occurred late in the burial history and were responsible for most of the secondary porosity in reservoir sandstones. Three mechanisms—undersaturated meteoric water, organic acids and (or) CO_2 derived from organic matter, and inorganic mineral reactions—might have caused the formation of secondary porosity. The first two are the most plausible mechanisms of dissolution. Leaching of carbonate by through-flowing meteoric waters probably was important at shallow depths and locally may have been of major importance; however, upon significant burial, meteoric flow most likely was not an important factor in secondary porosity development. In the deeper subsurface, the leaching capacity of low-acidity meteoric waters tends to be limited because the carbonate undersaturation is neutralized by reactions in the initial flow paths (Giles and Marshall, 1986; Giles, 1987). The exceptions are areas where well-developed fracture porosity may have helped to distribute undersaturated water over a larger distance than would have been possible if flow occurred through the pore network alone. The geochemical characteristics of petroleum in sandstones suggest that meteoric water was not a major factor in the mineral dissolution process during the time of hydrocarbon migration. Crude oils consistently have high API gravities ($\sim 30^\circ$ – 45°) and water-soluble, saturated compounds are preserved (Hatch and others, 1991), indicating that there was virtually no biodegradation or water washing of the hydrocarbons. This is the opposite of what would be expected if there had been large meteoric fluxes late in the basin's burial history.

Inasmuch as sandstones within the Bethel-Cypress interval are among the principal reservoirs for hydrocarbons in the basin, it follows that organic acids and CO_2 produced during the early stages of hydrocarbon generation might have played a role in carbonate-cement and feldspar dissolution (Burley and others, 1985; Surdam and others, 1984). Carothers and Kharaka (1978) showed that short-chain organic acids can be present in formation waters throughout the 80° – 200°C temperature range, assuming there has been no mixing with meteoric waters or dilution from deeper, hotter waters. The carboxylic acid anion dominance is particularly pronounced at temperatures of 80° – 120°C and can buffer the alkalinity to relatively low pH values at low P_{CO_2} , which increases carbonate solubility (Surdam and Crossey, 1987; Crossey and others, 1986). The reconstructed burial-thermal history suggests that inorganic diagenesis and mineral dissolution in sandstones within the Bethel and Cypress spanned a temperature range of $\sim 30^\circ$ – 140°C (fig. 14). Although no direct proof of the involvement of organic acids in the dissolution of carbonate cement is available, the temperature interval coincident with calcite dissolution ($\sim 90^\circ$ – 120°C) overlaps the thermal window in which the

maximum concentrations of organic acids are produced during the early stages of hydrocarbon generation (80°–120°C) and thus provides support for the role of organic acids in secondary-porosity development.

Clay-carbonate reactions have been recognized as potential agents of mineral dissolution in many basins (Crossey and others, 1986; Lundegard and Land, 1986). In sandstones within the Bethel-Cypress interval, kaolinite is sparse, but, if it previously was common in the more thermally mature sandstones, its general absence may be due to clay/carbonate reactions (i.e., kaolinite-calcite and (or) kaolinite-ankerite) that largely eliminated the kaolinite. The volume of secondary porosity that can be generated from such mineral reactions was not calculated because the initial abundances of kaolinite are not known.

Selective K-feldspar leaching might be related to smectite/illite transformations in finer grained sandstones. Illitization of smectite takes place at temperatures of 70°–100°C (Hower and others, 1976; Pollastro, 1993). However, in this temperature range, the potassium uptake caused by smectite-to-illite conversion is much slower than the potassium released by K-feldspar dissolution, implying that the rate of K-feldspar dissolution should not be the rate-limiting factor in illitization of smectite (Altaner, 1986). The illite content in sandstones with high secondary porosity within the Bethel-Cypress interval does not exceed a few percent, and interstratified illite/smectite is insignificant; therefore, illitization of smectite may not have been associated with K-feldspar dissolution in sandstones. Upon dissolution of feldspar, aluminum is released, but due to its very low solubility (and mobility), aluminum must be consumed locally if dissolution is to proceed.

GENERATION AND MIGRATION OF PETROLEUM

Textural relations indicate that hydrocarbon entrapment is the latest diagenetic event that occurred in the Bethel and Cypress Sandstones (fig. 14). The origin of hydrocarbon residue in secondary pores has not been studied specifically, but it is best explained as the result of migrated oil sourced from the Upper Devonian to Lower Mississippian New Albany Shale, which underlies the Chesterian Series by ~300 m (Swann, 1963). In the southern part of the Illinois Basin, hydrocarbon generation and migration in the New Albany started in the Middle to Late Pennsylvanian and reached their peak in the Early Permian when Upper Mississippian sandstones were close to their maximum burial depths and temperatures (Cluff and Byrnes, 1991). Generation and migration occurred later in the central part of the basin where the rocks were less deeply buried.

Most of the hydrocarbon production in sandstones within the Bethel-Cypress interval is concentrated along major structural features and faults, with many of the larger

reservoirs situated in the west-central part where sandstones have the best reservoir quality. The majority of the hydrocarbons reside in combination traps that overlie the generative portion of the basin (M. Lewan, 1997, unpub. data), which indicates that petroleum migrated vertically, primarily by buoyancy, along normal (extensional) faults and fractures with focused lateral flow locally updip where vertical flow paths intersected porous and permeable sandstone beds. Unconformity surfaces may have supplemented the primary migration pathways, especially in the center of the basin. Studies by Kolata and Nelson (1991) show that many of the major folds and faults that served as major conduits for hydrocarbon transport formed during or prior to hydrocarbon generation and expulsion in the Late Pennsylvanian and Early Permian. In southern Illinois and in the northern Reelfoot rift area, a period of igneous activity coupled with a brief but intense hydrothermal fluid-flow event accompanied late Paleozoic tectonism (Bethke, 1986). The exceptionally high rates of heat flow associated with the igneous activity and the advecting hydrothermal fluids resulted in temperatures exceeding those of normal burial in Upper Mississippian sandstones (see fig. 14). Presumably this high heat pulse also increased the rate of hydrocarbon expulsion in mature New Albany source rocks, which could account for the large volumes of petroleum that accumulated in late Paleozoic (and older) structures over a relatively short time period, approximately 60 m.y. (Abrams, 1995).

It is noteworthy that petroleum migration and Mississippi Valley-type mineralization were contemporaneous in southern Illinois. In the Illinois/Kentucky Fluorspar district, abundant oil in fluid inclusions within sphalerite and fluorite, and bitumen coating gangue minerals in fractures, are evidence that petroleum was present at the time of mineralization in the mid Permian (~270 Ma; Richardson and Pinkney, 1984; Richardson and others, 1988; Chesley and others, 1994). The temporal and spatial relationship between hydrocarbons and ore minerals indicate that the hydrocarbons migrated along the same fault and fracture systems that served as conduits for the mineralizing fluids. However, the discontinuous nature of individual reservoir units and the predominance of oil in traps overlying mature New Albany source rocks (Lewan, 1997, unpub. data) suggest that hydrothermal ore-forming fluids were not an important driving mechanism for oil migration in the basin as was previously thought (Bethke and others, 1991).

THERMAL AND HYDROLOGIC CONTROLS ON DIAGENESIS

Petrographic, stable-isotope and fluid-inclusion data provide good evidence for mixing of fluids of different temperatures from different sources during diagenesis in southern Illinois. The oxygen-isotopic evolution of pore water

suggests a rather constant composition during early non-ferroan carbonate (and quartz) precipitation, followed by a shift to relatively heavy values during late-stage ferroan carbonate and fracture cementation. Occurrences of early-diagenetic quartz overgrowths and syntaxial calcite and planar dolospar indicate precipitation at low to moderate temperatures in a meteoric-water-dominated, shallow-burial regime. In contrast, late-stage cements, including planar ankerite, saddle ankerite, and fracture-fill ferroan calcite, are compatible with precipitation from high-temperature, saline pore fluids in a system influenced by hydrothermal fluid flow. The strongest evidence for a hot, saline fluid source is based on a study of the Middle Ordovician St. Peter Sandstone in the Illinois Basin (Pitman and Spötl, 1996). Pitman and Spötl (1996) show that many of the petrographic and geochemical characteristics of burial-related carbonate cements in Ordovician sandstones resemble those of late-diagenetic carbonate cements in Mississippian sandstones, suggesting they may be genetically related. For example, saddle dolomite in the St. Peter Sandstone precipitated at minimum temperatures of $\sim 140^{\circ}\text{C}$; planar ankerite and saddle ankerite in sandstones within the Bethel-Cypress interval precipitated at about the same temperatures, $\sim 120^{\circ}\text{--}140^{\circ}\text{C}$. The stable-isotope geochemistry of these phases also is broadly comparable. In the St. Peter, $\delta^{13}\text{C}$ values vary from ~ 3 to -8‰ and $\delta^{18}\text{O}$ values vary from ~ 5 to -8‰ ; $\delta^{13}\text{C}$ and $\delta^{18}\text{O}$ values in the Bethel and the Cypress overlap this range, varying from ~ 0 to -9‰ and ~ 5 to -12‰ , respectively. Oxygen-isotope modeling coupled with fluid-inclusion analysis demonstrated that precipitating waters at minimum temperatures of 140°C in the St. Peter were highly saline (>20 weight percent NaCl equivalent), with $\delta^{18}\text{O}$ values ranging from ~ 3 to 9‰ (Pitman and Spötl, 1996). Pore-fluid compositions predicted at temperatures of $120^{\circ}\text{--}140^{\circ}\text{C}$ in the Bethel and the Cypress fall in the same range ($\delta^{18}\text{O} = \sim 0$ to 9‰ SMOW), suggesting that the high-temperature, saline fluids that precipitated burial cements in Ordovician sandstones also may have formed ankerite in Mississippian sandstones.

The precipitation of late-diagenetic cements in Mississippian and Ordovician sandstones overlaps the timing of late Paleozoic tectonism and hydrothermal fluid migration in the Illinois Basin, which has been broadly constrained to have occurred during the Late Pennsylvanian and Early Permian. Thermal models show that the basin as a whole was affected by the influx of hot fluids and that transport of heat by these fluids significantly elevated the basin's thermal regime for a period of about 200,000 years (Rowan and Goldhaber, 1995). The change in fluid-flow dynamics in the basin to an advective, hydrothermal-flow system most likely was related to a change in the stress regime imposed by the Ouachita orogeny in the Late Pennsylvanian and Early Permian. During this time, gravity-driven recharge in the Appalachian-Ouachita highlands drove hot fluids from the deep Arkoma Basin northward through the Reelfoot rift and updip into the Illinois Basin proper (Bethke and others, 1988;

Bethke and Marshak, 1990; Garven and others, 1993). Data presented in this study and in Pitman and others (1996) provide evidence to suggest that these fluids (and hydrocarbons) moved through the basin by cross-formational flow along major bounding faults into porous and permeable reservoir units. Late-diagenetic mineral assemblages that formed from these hot fluids are found mainly in areas where folds and faults intersect these units.

CONCLUSIONS

Reservoir quality variations in sandstones within the Bethel-Cypress interval were evaluated on the basis of whole-core analyses and petrographic characteristics. Porosity in sandstones varies from 10 to 25 percent and decreases systematically with greater depth of burial due to the effects of mechanical compaction and quartz and carbonate cementation. Permeability is a function of porosity as well as a number of other factors and ranges over several orders of magnitude ($<1\text{--}2,500$ mD) at any given depth. In the western part of the depositional area, porosity is highest and reflects preservation of initial pore space, enhanced by secondary porosity caused by leaching of framework grains and authigenic calcite cement. During shallow diagenesis, meteoric water was involved in the dissolution of calcite, but later, organic acids and CO_2 produced during the early stages of hydrocarbon generation promoted more extensive carbonate dissolution. Reservoir quality in drilled and prospective undrilled areas should differ little because stratigraphically equivalent sandstones formed in similar depositional environments, had the same framework-grain compositions, and were subject to the same porosity reduction and enhancement processes.

Diagenetic alteration in sandstones within the Bethel-Cypress interval commenced during the period of rapid sediment burial in the Late Mississippian and continued until migration of oil into sandstones in the Late Pennsylvanian and Early Permian. Major diagenetic events observed in sandstones include (1) precompactional illite and early chlorite precipitation, (2) early quartz, and calcite and dolomite cementation, (3) calcite-cement and framework-grain dissolution, (4) illite and kaolinite formation, (5) late quartz and ankerite precipitation, (6) fracture cementation, and (7) hydrocarbon emplacement. Syntaxial calcite, dolomicrospar, and quartz overgrowths formed during early burial at temperatures of $\sim 30^{\circ}\text{--}90^{\circ}\text{C}$ in a regime dominated by freshwater inflow. By the Late Pennsylvanian to Early Permian, when the rocks were near maximum burial (~ 2 km), planar ankerite, saddle ankerite, and minor quartz precipitated at temperatures as high as 140°C in a diagenetic system influenced by igneous heat and advective heat from tectonically driven, hydrothermal fluids. In southern Illinois, hydrocarbons expelled as a consequence of this high heat pulse moved updip along faults and fractures, forming large accumulations of petroleum in sandstone reservoirs.

ACKNOWLEDGMENTS

This study was supported by the U.S. Geological Survey's Energy Resources Program in cooperation with the State Geological Surveys of Illinois, Indiana, and Kentucky. Special thanks are extended to Marty Goldhaber for generating the burial-thermal curves used in the study. The authors also are indebted to Jennie Ridgley and Neil Fishman for reviewing the manuscript and providing helpful suggestions.

REFERENCES CITED

- Abrams, R.H., 1995, Long-range buoyancy-driven oil migration in the Illinois Basin: Stanford University. Ph.D. thesis, 78 p.
- Altaner, S.P., 1986, Comparison of rates of smectite illitization with rates of K-feldspar dissolution: Clays and Clay Minerals, v. 34, p. 608–611.
- Atkins, J.E., and McBride, E.F., 1992, Porosity and packing of Holocene river, dune, and beach sands: American Association of Petroleum Geologists Bulletin, v. 76, p. 339–355.
- Baldwin, B., and Butler, C.O., 1985, Compaction curves: American Association of Petroleum Geologists Bulletin, v. 69, p. 622–626.
- Beard, D.C., and Weyl, P.K., 1973, Influence of texture on porosity and permeability of unconsolidated sand: American Association of Petroleum Geologists Bulletin, v. 57, p. 349–369.
- Bethke, C.M., 1986, Hydrologic constraints on the genesis of the Upper Mississippi Valley mineral district from Illinois Basin brines: Economic Geology, v. 81, p. 233–249.
- Bethke, C.M., Harrison, W.J., Upson, C., and Altaner, S.P., 1988, Supercomputer analysis of sedimentary basins: Science, v. 239, p. 261–267.
- Bethke, C.M., and Marshak, S., 1990, Brine migration across North America: The plate tectonics of groundwater: Annual Review of Earth Planetary Science, v. 18, p. 287–315.
- Bethke, C.M., Reed, J.D., and Oltz, D.F., 1991, Long-range petroleum migration in the Illinois Basin, in Leighton, M.W., Kolata, D.R., Oltz, D.F., and Eidel, J.J., eds., Interior Cratonic Basins: American Association of Petroleum Geologists Memoir 51, p. 455–472.
- Bjorlykke, K., and Egeberg, P.K., 1993, Quartz cementation in sedimentary basins: American Association of Petroleum Geologists Bulletin, v. 77, p. 1538–1548.
- Boles, J.R., and Franks, S.G., 1979, Clay diagenesis in Wilcox sandstones of southwest Texas: Implication of smectite diagenesis on sandstone cementation: Journal of Sedimentary Petrology, v. 49, p. 55–70.
- Brewer, R., 1976, Fabric and Mineral Analysis of Soils: New York, John Wiley and Sons, 470 p.
- Burley, S.D., Kantorowicz, J.D., and Waugh, J., 1985, Clastic diagenesis, in Brenchley, P.J., and Williams, B.P.J., eds., Sedimentology: Recent Developments and Applied Aspects: London, Geological Society of London, p. 189–225.
- Carothers, W.W., and Kharaka, Y.K., 1978, Aliphatic acid anions in oil-field waters—Implications for the origin of natural gas: American Association of Petroleum Geologists Bulletin, v. 62, p. 2441–2453.
- Chesley, J.T., Halliday, A.N., Kyser, T.K., and Spry, P.G., 1994, Direct dating of Mississippi Valley-type mineralization: Use of Sm-Nd in fluorite: Economic Geology, v. 89, p. 1192–1199.
- Cluff, R.M., and Byrnes, A.P., 1991, Lopatin analysis of maturation and petroleum generation in the Illinois Basin, in Leighton, M.W., Kolata, D.R., Oltz, D.F., and Eidel, J.J., eds., Interior Cratonic Basins: American Association of Petroleum Geologists Memoir 51, p. 425–454.
- Crossey, L.J., Surdam, R.C., and Lahmann, R., 1986, Application of organic/inorganic diagenesis to porosity prediction, in Gautier, D.L., ed., Roles of Organic Matter in Sediment Diagenesis: Society of Exploration Paleontologists and Mineralogists Special Publication 38, p. 147–156.
- Damburger, H.H., 1971, Coalification pattern of the Illinois Basin: Economic Geology, v. 66, p. 488–494.
- Ehrenberg, S.N., 1995, Measuring sandstone compaction from modal analyses of thin sections: How to do it and what the results mean: Journal of Sedimentary Research, v. A64, p. 369–379.
- Folk, R.L., 1974, Petrology of Sedimentary Rocks: Austin, Texas, Hemphill, 182 p.
- Friedman, I., and O'Neil, J.R., 1977, Compilation of stable isotope fractionation factors of geochemical interest, in Fleischer, M., ed., Data of Geochemistry, 6th ed.: U.S. Geological Survey Professional Paper 440-KK, 12 p.
- Fritz, P., and Smith, D.C.W., 1970, The isotopic composition of secondary dolomite: Geochimica et Cosmochimica Acta, v. 34, p. 1161–1173.
- Garven, G., Ge, S., Person, M.A., and Sverjensky, D.A., 1993, Genesis of stratabound ore deposits in the Midcontinent basins of North America. I. The role of regional groundwater flow: American Journal of Science, v. 293, p. 497–568.
- Giles, M.R., 1987, Mass transfer and problems of secondary porosity creation in deeply buried hydrocarbon reservoirs: Marine and Petroleum Geology, v. 4, p. 188–204.
- Giles, M.R., and Marshall, J.D., 1986, Constraints on the development of secondary porosity in the subsurface: Reevaluation of processes: Marine and Petroleum Geology, v. 3, p. 243–255.
- Hatch, J.R., Risatti, J.B., and King, J.D., 1991, Geochemistry of Illinois Basin oils and hydrocarbon source rocks, in Leighton, M.W., Kolata, D.R., Oltz, D.F., and Eidel, J.J., eds., Interior Cratonic Basins: American Association of Petroleum Geologists Memoir 51, p. 403–423.
- Heald, M.T., 1955, Stylolites in sandstones: Journal of Geology, v. 63, p. 101–114.
- Houseknecht, D.W., 1984, Influence of grain size and temperature on intergranular pressure solution, quartz cementation, and porosity in a quartzose sandstone: Journal of Sedimentary Petrology, v. 54, p. 348–361.
- 1987, Assessing the relative importance of compactional processes and cementation to the reduction of porosity in sandstones: American Association of Petroleum Geologists Bulletin, v. 71, p. 633–642.
- 1988, Intergranular pressure solution in four quartzose sandstones: Journal of Sedimentary Petrology, v. 58, p. 228–246.
- Hower, J., Eslinger, E.V., Hower, M.E., and Perry, E.A., 1976, Mechanism of burial metamorphism of argillaceous sediments. I—Mineralogical and chemical evidence: American Association of Petroleum Geologists Bulletin, v. 87, p. 725–737.

- Kolata, D.R., and Nelson, W.J., 1991, Tectonic history of the Illinois Basin, *in* Leighton, M.W., Kolata, D.R., Oltz, D.F., and Eidel, J.J., eds., Interior Cratonic Basins: American Association of Petroleum Geologists Memoir 51, p. 263–285.
- Lundegard, P.D., and Land, L.S., 1986, CO₂ and organic acids: Their role in porosity enhancement and cementation, Paleogene of the Texas Gulf Coast, *in* Gautier, D.L., ed., Roles of Organic Matter in Sediment Diagenesis: Society of Exploration Paleontologists and Mineralogists Special Publication 38, p. 128–146.
- Meyers, W.J., and Lohmann, K.C., 1985, Isotope geochemistry of regionally extensive calcite cement zones and marine components in Mississippian limestones, New Mexico, *in* Schneidermann, N., and Harris, P.M., eds., Carbonate Cements: Society of Economic Paleontologists and Mineralogists Special Publication 36, p. 223–239.
- Pitman, J.K., and Spötl, C., 1996, Origin and timing of carbonate cements in the St. Peter Sandstone, Illinois Basin: Evidence for a genetic link to Mississippi Valley-type mineralization, *in* Crossey, L.J., Loucks, R., and Totten, M.W., eds., Siliciclastic Diagenesis and Fluid Flow: Concepts and Applications: Journal of Sedimentary Geology Special Publication 55, p. 187–202.
- Pollastro, R.M., 1993, Considerations and applications of the illite/smectite geothermometer in hydrocarbon-bearing rocks of Miocene to Mississippian age: Clays and Clay Minerals, v. 41, p. 119–133.
- Pryor, W.A., Lambourg, A.D., Roberts, M.J., Tharp, T.C., and Wilsey, W.L.M., 1991, Geologic controls on porosity in Mississippian limestone and sandstone reservoirs in the Illinois Basin, *in* Leighton, M.W., Kolata, D.R., Oltz, D.F., and Eidel, J.J., eds., Interior Cratonic Basins: American Association of Petroleum Geologists Memoir 51, p. 329–359.
- Pryor, W.A., and Sable, E.G., 1974, Carboniferous of the Eastern Interior Basin: Geological Society of America Special Paper 148, p. 281–313.
- Richardson, C.K., and Pinkney, D.M., 1984, The chemical and thermal evolution of the fluids in the Cave-in-Rock Fluorspar district, Illinois: Mineralogy, paragenesis, and fluid inclusions: Economic Geology, v. 79, p. 1833–1856.
- Richardson, C.K., Rye, R.O., and Wasserman, M.D., 1988, The chemical and thermal evolution of the fluids in the Cave-in-Rock Fluorspar district, Illinois: Stable isotope systematics at the Deardorff mine: Economic Geology, v. 83, p. 765–783.
- Rowan, E.L., and Goldhaber, M.B., 1995, Duration of mineralization and fluid-flow history of the Upper Mississippi Valley zinc-lead district: Geology, v. 23, p. 609–612.
- Rowan, E.L., Goldhaber, M.B., and Hatch, J.R., in press, The role of regional fluid flow in the Illinois Basin's thermal history: Constraints from fluid inclusions and the maturity of Pennsylvanian coals: American Association of Petroleum Geologists Bulletin.
- Siever, R., 1962, Silica solubility, 0–200°C, and the diagenesis of siliceous sediments: Journal of Geology, v. 70, p. 127–150.
- Stone, W.N., and Siever, R., 1994, The making of quartzite: Where is the quartzose sandstone porosity basement? [abs.]: American Association of Petroleum Geologists: 1994 Annual Convention Program, v. 3, p. 265.
- Stone, W.N., Siever, R., and Paxton, S.T., 1993, Compaction and quartz cementation in quartzarenites and subarkoses from the Greater Green River, Anadarko, and East Texas Basins [abs.]: Geological Society of America, Abstracts with Programs, v. 25, no. 6, p. A-65.
- Sullivan, D.M., 1972, Subsurface stratigraphy of the West Baden Group in Indiana: Indiana Geological Survey Bulletin 47, 31 p.
- Surdam, R.C., Boese, S.W., and Crossey, L.J., 1984, The chemistry of secondary porosity, *in* Surdam, R.C., and McDonald, P.A., eds., Clastic Diagenesis: American Association of Petroleum Geologists Memoir 37, p. 151–162.
- Surdam, R.C., and Crossey, L.J., 1987, Integrated diagenetic modeling: A process-oriented approach for clastic systems: Annual Reviews, Earth and Planetary Sciences, v. 15, p. 141–170.
- Surdam, R.C., Crossey, L.J., Hagen, E.S., Heasler, H.P., 1989, Organic-inorganic interactions and sandstone diagenesis: American Association of Petroleum Geologists Bulletin, v. 73, p. 1–23.
- Swann, D.H., 1963, Classification of Genevievian and Chesterian (Late Mississippian) rocks of Illinois: Illinois State Geological Survey Report of Investigations 216, 91 p.
- 1967, A summary geological history of the Illinois Basin, *in* Geology and Petroleum Production of the Illinois Basin: Illinois Geological Society, p. 3–21.
- Treworgy, J.D., 1991, Kaskaskia sequence: Mississippian and Valmeyeran Series, *in* Leighton, M.W., Kolata, D.R., Oltz, D.F., and Eidel, J.J., eds., Interior Cratonic Basins: American Association of Petroleum Geologists Memoir 51, p. 125–142.
- Weyl, P.K., 1959, Pressure solution and the force of crystallization—A phenomenological theory: Journal of Geophysical Research, v. 64, p. 2001–2025.
- Walters, L.J., Claypool, G.E., and Choquette, P.W., 1972, Reaction rates and $\delta^{18}\text{O}$ variation for the carbonate-phosphoric acid preparation method: Geochimica et Cosmochimica Acta, v. 36, p. 129–140.
- Willman, H.B., Atherton, E., Buschbach, T.C., Collinson, C., Frye, J.C., Hopkins, M.E., Lineback, J.A., and Simon, J.A., 1975, Handbook of Illinois stratigraphy: Illinois State Geological Survey Bulletin 95, 261 p.

Published in the Central Region, Denver, Colorado
 Manuscript approved for publication February 11, 1998
 Edited by Richard W. Scott, Jr.
 Graphics preparation and photocomposition by
 Carol A. Quesenberry

Selected Series of U.S. Geological Survey Publications

Books and Other Publications

Professional Papers report scientific data and interpretations of lasting scientific interest that cover all facets of USGS investigations and research.

Bulletins contain significant data and interpretations that are of lasting scientific interest but are generally more limited in scope or geographic coverage than Professional Papers.

Water-Supply Papers are comprehensive reports that present significant interpretive results of hydrologic investigations of wide interest to professional geologists, hydrologists, and engineers. The series covers investigations in all phases of hydrology, including hydrogeology, availability of water, quality of water, and use of water.

Circulars are reports of programmatic or scientific information of an ephemeral nature; many present important scientific information of wide popular interest. Circulars are distributed at no cost to the public.

Fact Sheets communicate a wide variety of timely information on USGS programs, projects, and research. They commonly address issues of public interest. Fact Sheets generally are two or four pages long and are distributed at no cost to the public.

Reports in the **Digital Data Series (DDS)** distribute large amounts of data through digital media, including compact disc-read-only memory (CD-ROM). They are high-quality, interpretive publications designed as self-contained packages for viewing and interpreting data and typically contain data sets, software to view the data, and explanatory text.

Water-Resources Investigations Reports are papers of an interpretive nature made available to the public outside the formal USGS publications series. Copies are produced on request (unlike formal USGS publications) and are also available for public inspection at depositories indicated in USGS catalogs.

Open-File Reports can consist of basic data, preliminary reports, and a wide range of scientific documents on USGS investigations. Open-File Reports are designed for fast release and are available for public consultation at depositories.

Maps

Geologic Quadrangle Maps (GQ's) are multicolor geologic maps on topographic bases in 7.5- or 15-minute quadrangle formats (scales mainly 1:24,000 or 1:62,500) showing bedrock, surficial, or engineering geology. Maps generally include brief texts; some maps include structure and columnar sections only.

Geophysical Investigations Maps (GP's) are on topographic or planimetric bases at various scales. They show results of geophysical investigations using gravity, magnetic, seismic, or radioactivity surveys, which provide data on subsurface structures that are of economic or geologic significance.

Miscellaneous Investigations Series Maps or Geologic Investigations Series (I's) are on planimetric or topographic bases at various scales; they present a wide variety of format and subject matter. The series also includes 7.5-minute quadrangle photogeologic maps on planimetric bases and planetary maps.

Information Periodicals

Metal Industry Indicators (MII's) is a free monthly newsletter that analyzes and forecasts the economic health of five metal industries with composite leading and coincident indexes: primary metals, steel, copper, primary and secondary aluminum, and aluminum mill products.

Mineral Industry Surveys (MIS's) are free periodic statistical and economic reports designed to provide timely statistical data on production, distribution, stocks, and consumption of significant mineral commodities. The surveys are issued monthly, quarterly, annually, or at other regular intervals, depending on the need for current data. The MIS's are published by commodity as well as by State. A series of international MIS's is also available.

Published on an annual basis, **Mineral Commodity Summaries** is the earliest Government publication to furnish estimates covering nonfuel mineral industry data. Data sheets contain information on the domestic industry structure, Government programs, tariffs, and 5-year salient statistics for more than 90 individual minerals and materials.

The Minerals Yearbook discusses the performance of the worldwide minerals and materials industry during a calendar year, and it provides background information to assist in interpreting that performance. The Minerals Yearbook consists of three volumes. Volume I, Metals and Minerals, contains chapters about virtually all metallic and industrial mineral commodities important to the U.S. economy. Volume II, Area Reports: Domestic, contains a chapter on the minerals industry of each of the 50 States and Puerto Rico and the Administered Islands. Volume III, Area Reports: International, is published as four separate reports. These reports collectively contain the latest available mineral data on more than 190 foreign countries and discuss the importance of minerals to the economies of these nations and the United States.

Permanent Catalogs

"Publications of the U.S. Geological Survey, 1879–1961" and **"Publications of the U.S. Geological Survey, 1962–1970"** are available in paperback book form and as a set of microfiche.

"Publications of the U.S. Geological Survey, 1971–1981" is available in paperback book form (two volumes, publications listing and index) and as a set of microfiche.

Annual supplements for 1982, 1983, 1984, 1985, 1986, and subsequent years are available in paperback book form.